Measuring residual strain and stress in thermal spray coatings using neutron diffractometers

N. H. Faisal[a,1], R. Ahmed[b], A. K. Prathuru[a], A. Paradowska[c,d], T. L. Lee[e]

[a] *School of Engineering, Robert Gordon University, Garthdee Road, Aberdeen, AB10 7GJ, UK*

[b] *School of Engineering and Physical Sciences, Heriot-Watt University, Edinburgh, EH14 4AS, UK*

[c] *Australian Nuclear Science and Technology Organisation, Lucas Heights, NSW 2234, Australia*

[d] *School of Civil Engineering, The University of Sydney, Sydney, NSW 2006, Australia*

[e] *ISIS Neutron Source, Science and Technology Facilities Council (STFC), Rutherford Appleton Laboratory, Didcot, OX11 0QX, UK*

Abstract

During thermal spray coating, residual strain (or stress) is formed within the coating and substrates due to many processes (quenching stress, peening effect, deposition temperature, lamella structure) and microstructural phase changes. It is also known that the residual stress values of thermally sprayed coatings are dependent upon the measurement method. Neutron diffraction technique can provide a non-destructive through-thickness residual strain analysis in thermally sprayed components with a level of detail not normally achievable by other techniques. Despite this advantage, the number of studies involving neutron diffraction analysis in thermal spray coatings remain limited, partly due to the limited number of neutron diffraction strain measurement facilities globally, and partly due to the difficulty is applying neutron diffraction analysis to measure residual strain in the complex thermal spray coating microstructure. This paper provides a comprehensive guide to researchers planning to use this technique for thermal spray coatings, and reviews some of these studies. ENGIN-X at the ISIS spallation source in the UK is a neutron diffractometer (time-of-flight) dedicated to materials science and engineering with high resolution and versatile capabilities. The focus is on the procedure of using ENGIN-X diffractometer for thermal spray coatings with a view that it can potentially be translated to other neutron diffractometers. Neutron sources worldwide (e.g. Africa, Asia, Australia, Europe, and North America) have been used to measure strains in various materials, and here, we present few examples where thermal spray coatings have been characterised at various neutron sources worldwide, to study the residual strains and microstructures.

Keywords: Residual strain, residual stress, neutron diffraction techniques, thermal spray coatings, ENGIN-X, neutron diffractometers

[1] Corresponding authors. E-mail addresses: N.H.Faisal@rgu.ac.uk; Tel: +44 (0) 1224-26 2438.

Electronic copy available at: https://ssrn.com/abstract=3711244

1. Introduction

This paper presents test methodologies for experimentally determining residual strain (and stress) in thermal spray coatings neutron diffraction technique with emphasis on ENGIN-X diffractometer at the ISIS neutron source in the UK [1]. The techniques presented here can potentially be applied to other neutron diffractometers, available globally, for the measurement of residual strain in thermal spray coatings. Although the physics of neutron diffraction remains the same, the availability of strain measurement instrumentation at different neutron diffractometers varies globally and requires adjustments for a comprehensive strain analysis. Nevertheless, the high resolution of through-thickness non-destructive residual strain analysis, if planned and performed carefully using neutron diffraction, is not normally achievable by other experimental techniques. This guide can apply to all thermal spray coating and substrate systems and intended to measure through-thickness microscopic residual strain that uses the measurement of the positions of the diffracted neutron spectra peaks to determine changes in the lattice spacing.

Thermal spray coating processes involve the build-up of a layer of partially molten splats which are heated and propelled by a spray (a flame or plasma, see **Fig. 1(a)**) towards a substrate. Difference between coatings obtained through a single pass and multiple passes is shown in **Fig. 1(b)**. The relevant differences are: (a) thicker substrate, (b) higher temperature seen on the substrate, and (c) the substrate is of a different material. Thermal spray processes are characterized by residual strain (or stress) within the coating and substrates due to different physical phenomena (quenching stress, peening effect, deposition temperature, lamella structure) and phase transformations [2-6], **Fig. 1(c)**. That residual stresses dictate the quality and performance (e.g. adhesion, fatigue, tribological behaviour [3]) of the coating substrate system (with coating thicknesses ranging from 50-500 μm) is a well-established fact. Measurement of residual stress is therefore crucial to evaluate and quantify coatings quality.

The measurement method dictates the residual stress measured within a thermally sprayed coating (or any other material). Non-destructive (laboratory X-ray, synchrotron X-ray, neutron (e.g. **Fig. 2**), Raman spectroscopy, digital image correlation, photoluminescence piezospectroscopy), semi-destructive (hole-drilling & ring-coring, layer removal, focused ion beam milling, indentation), and miscellaneous other (curvature, modified layer removal, material removal, diametral compression) approaches have been adapted to experimentally evaluate the residual stress fields in thermal spray coatings. The lifetime of the coating system is very much dependent on the residual stress and this is dependent on the measurement method. This dependency on the measurement method directly influences the verification of numerical and

Electronic copy available at: https://ssrn.com/abstract=3711244

experimental models used to predict the residual stress evolution within the coating systems. Hence what is important and is lacking within the existing literature is the comparative study of the various destructive and non-destructive methods of through thickness residual stress measurement, though studies exist on the use of a single method [4].

Non-destructive measurement of these strain (or stress) fields in relatively thin thermal spray coatings is also technologically challenging, because techniques such as deep hole drilling, laboratory X-ray, synchrotron X-ray and beam curvature methods are either destructive and/or provide only a sub-surface strain measurement. Where the very-near surface residual stresses play a critical role, e.g. surface crack initiation due to wear, surface roughness effects complicate the surface residual stress measurements. Particularly in the case of thermal spray coatings, techniques such as X-ray and synchrotron X-ray can only provide a through thickness residual stress measurement through a destructive process (layer-removal process). Accordingly, recent investigations have concentrated on the use of various non-destructive techniques (e.g. diffraction, optical spectroscopy) for such strain analysis.

In this work, a practical example of the test method at room temperature and unloaded condition was presented with some of the recent findings of through-thickness residual strain measurements in as-sprayed coatings via the ENGIN-X neutron diffraction instrument. We also present few examples where thermal spray coatings have been characterised at various neutron sources worldwide to study the residual strains and microstructures.

2. Origin of residual stresses in thermal spray coating

Residual stresses occur in the material or components at the removal of any external loads (e.g. applied force, displacement, thermal) during manufacturing or service loading [7-8]. These stresses are locked inside the material and are superimposed on stresses subsequent service loading or manufacturing. Residual stresses in thermal spray coatings can have different magnitude and distribution, depending on the combination of coating and substrate materials and processing conditions. These stresses can also be altered due to service loading and/or thermal heat-treatment of the coating substrate system. A certain level of compressive residual stress in the coating material is always desirable to resist crack initiation/propagation and coating degradation during service loading. Very high compressive residual stress in coating is however not desired [9-14].

As the coating performance during service loading depends on the structure-property relationships, such as microstructural phases, hardness, fracture toughness, anisotropy and other microstructural features, it is not always possible to design the optimum residual stress profile in the given coating substrate system. Functional grading

Electronic copy available at: https://ssrn.com/abstract=3711244

of the coating, where the composition of coating microstructure is varied through thickness, either uniformly, or by depositing layers of different materials can sometimes be used to improve the residual stress profile to combat coating delamination. Formation of residual stress is inherent to the nature of thermal spray coating process. These stresses can be caused by quenching stress, peening effect, deposition temperature and phase transformations. Based on physical and metallurgical phenomena dictating the residual strain behaviour, through thickness residual strain profile of thermal spray coating is influenced by the following four major factors [6]:

(a) *Role of quenching stress:* The quenching stresses, which appear within individual splats, are caused due to the constriction of the contraction of the individual splat by the lamellae lying underneath that are created due to the preceding spray pass. The degree of constrained contraction is a function of the individual splat temperature and the size of powder particles. Quenching stresses are always tensile as the contraction of splat or lamella during its rapid cooling is constrained by the underlying deposit at relatively lower temperature, means deposited splats thermal contraction after solidification is constrained by the underlying solid splats. Hence the magnitude of quenching stress is a function of ratio of the deposition temperature of the powder particle and its melting point.

(b) *Peening effect*: The high particle velocity seen in thermal spray processes is known to have a peening effect which results in compressive residual stresses in the coating. Hence the peening stress is a function of the momentum of the powder particle during thermal spraying, i.e. the deposition velocity and the mass of the powder particle and the temperature-dependent plasticity of the underlying deposit. The mechanism is like the shot-peening of gears and shafts as an engineering practice to induced compressive residual stress to combat fatigue and fracture. Hence, thermal spray coating processes such as the high velocity oxy-fuel (HVOF) process, with relatively high particle velocities are understood to cause relatively high compressive residual stresses in the coatings.

(c) *Role of deposition temperature:* Macro residual stress occurs due to the differences in the coefficient of thermal expansion (*CTE*) of coating and substrate materials. These stresses can be compressive or tensile depending upon the mismatch of the *CTE* of the coating and substrate materials, e.g. if $CTE_{coating} > CTE_{substrate}$, the stress in the coating will be tensile as its contraction is constrained.

(d) *Phase transformation*: The cooling of impacting powder particle or lamella occurs in a matter of few micro-seconds from a near-molten temperature to form a solid deposit. This can lead to amorphous phases in the coating material depending upon the temperature of the impacting lamella. There is not enough time for

Electronic copy available at: https://ssrn.com/abstract=3711244

crystal structures to form in a fully molten powder particle, so it is desirable to control the heating of powder particle to near-melting point but not above it. There is also a possibility of oxidation of powder materials in some cases leading to further phase transformations. Some of these phase transformations can lead to a small volume change in the crystal structure. This change in volume can provide an accommodation mechanism at inter-splat boundaries for the coatings, leading to residual strain.

Overall, the residual stress in thermal spray coatings is a function firstly of the distribution of temperature and velocity of individual powder particles in the spray stream. Not all sprayed powder particles have the same temperature or velocity, which is a function of the location of the powder particle within the spray-stream during thermal spraying. Secondly, the residual formation is a function of the thermo-mechanical properties of the coating-substrate system, the most important being the temperature-dependent *CTE* characteristics and temperature-dependent elastic-plastic behaviour. Although, it is possible to model crudely the evolution of residual stress generation during thermal spraying using numerical modelling, but these numerical techniques are unable to accurately comprehend the variation of stress or account for phase transformations [15]. Multiscale modelling to combat some of these limitations makes the modelling approach computationally expensive. Hence, non-destructive experimental residual stress measurement remains critical for the evaluation of coating quality and predicting the service life of components.

3. Principle of neutron diffraction

Neutrons interact directly with the nucleus of the atom in a given material [16-19] instead of the electron cloud which significantly increases the penetration depth of neutrons for strain measurements. Since neutron of all energies is produced in a short pulse, the de Broglie's relation given momentum (p) and hence neutron speed (v) is given by [16]:

$$p = m_n v = \frac{h}{\lambda} \quad (1)$$

where, $m_n = 1.67 \times 10^{-27} kg$ is neutron mass, $h = 6.63 \times 10^{-34} Js$ is Planck's constant. Since neutron travels down the flight path (L) (e.g. 10 m to 100 m), to separate neutrons in time, therefore, time (T) of arrival at the detector is given by [16]:

$$T = \frac{L}{v} = \lambda\left(\frac{m_n L}{h}\right) \quad (2)$$

Neutron diffraction method, as with X-ray diffraction methods, measures the Bragg angle of scatter radiation using the equation (**Fig. 3**) [16]:

$$n\lambda = 2d_{hkl} sin\,\theta_{hkl} \quad (3)$$

Electronic copy available at: https://ssrn.com/abstract=3711244

where n is a positive integer, λ is the wavelength of the incident wave, d_{hkl} is the inter-planar spacing, (hkl) is the Miller indices, θ_{hkl} is one half of the angle through which the incident beam is diffracted by planes, which is related to the spacing between crystallographic planes. Hence, peaks are measured at times (T) given after the initial pulse given by [16]:

$$T = d_{hkl}\left(\frac{2m_n L sin\,\theta_{hkl}}{h}\right) \quad (4)$$

Each peak corresponds to an (*hkl*) family of lattice planes is given by Bragg's law. Like the X-ray diffraction method, the accuracy of the neutron diffraction method is dependent on the knowledge of spacing of the unstressed lattice of the crystallographic planes. This is because the stress is tri-axial at depth [19]. Similar to the synchrotron X-ray method, spacing at the measurement point in an unstressed lattice should be known but is not easy to measure. The neutron diffraction method shows a smaller range of scattering than X-ray diffraction which is another contributing factor to why it can penetrate deeper. A typical wavelength for neutron diffraction will range between 0.7 Å and 3 Å, and can measure the elastic strains caused residual stress by component thickness varying between 0.1 m and 1.5 m to less than 1 mm. This means the bulk residual stress within the component can be examined in a non-destructive manner.

Neutron diffraction strain measurements at the UK ISIS Facility utilises ENGIN-X strain measurement diffractometer, which is a pulsed neutron diffractometer equipped with slits and collimators to achieve small gauge volumes [17]. At ENGIN-X, the residual strain in the coating and substrate materials can be obtained from the shift in individual peaks (e.g. scheme shown in **Fig. 3(b)**) using a single or multiple peak fitting routine. Peaks with little to no overlap with others can be chosen for the strain analysis. The feedstock powder material or the powder obtained by carefully removing the coating from the substrate and crushing it can be used to measure the strain-free lattice parameter (d_{hkl}^0) for the coating material. This powder can then be put in a vanadium tube (which is transparent to neutrons) and its lattice parameter measured. The substrate strain free lattice parameter can then be measured at the free surface. The direct elastic strain (average) in the material at the measured direction can be calculated from the following [17]:

$$\varepsilon_{hkl} = \frac{d_{hkl} - d_{hkl}^0}{d_{hkl}^0} = \frac{\Delta d}{d_{hkl}^0} \quad (5)$$

where $d_{hkl}$is the measured interplanar lattice spacing and d_{hkl}^0 is the stress-free interplanar spacing for the material. The strain is measured in the direction of the scattering vector (**Fig. 3**). The elastic stress can be calculated from these strain values using the through-thickness (coating and substrate) elastic modulus values or Hooke's law:

Electronic copy available at: https://ssrn.com/abstract=3711244

$$\sigma_{ij} = \frac{E_{hkl}}{1+\upsilon_{hkl}}\left(\varepsilon_{ij} + \frac{\upsilon_{hkl}}{1-2\upsilon_{hkl}}\varepsilon_{qq}\delta_{ij}\right) \quad (6)$$

where σ_{ij} is stress calculated for a particular direction, E_{hkl} is the elastic coefficient for hkl plane, and υ_{hkl} is Poisson's ratio for hkl.

4. ENGIN-X neutron diffractometer

The ISIS spallation neutron sources (monochromatic incident beam), producing approximately 2 x 10^{18} fast neutrons per second as a frequency of 50 Hz with pulses of <1 μs in width with a 200 μA, 800 MeV proton current impinges on a tantalum (Ta) target [18]. As summarised by Zhang *et al.* [1], ENGIN-X has a variety of sample equipment to alter the experimental conditions. A specimen mounting stage assembles the specimen within the neutron beam path to allow strain measurements. The sample is aligned with the neutron beam with the help of a robotic arm. An in-situ mountable servo-hydraulic stress rig can apply up to ±100 kN cyclic loads to test the samples under various mechanical loading conditions, The rig can be maintained at a low or elevated temperature within the normal atmosphere or under inert gas using a furnace or a cryogenic rig. . The sample mounting stage allows samples weighting up to 1 tonne to be accurately positioned within the measurement point with the accuracy better than 10 μm. As an example, such mounting stages could be useful to assemble thermally sprayed large ball valves. The automated experimental setups for complex-shaped samples of various types can be addressed using a laser scanner and robotic arm metrology equipment in combination with the virtual measurement simulation software, SScanSS [20], creating digital geometry. Further details about the neutron strain measurement can be found in Schajer (2013) [19] and Hutchings *et al*. (2005) [21], including a description of the state-of-the-art in strain measurement using neutron radiation is presented by Fitzpatrick and Lodini [16] and about ENGIN-X by Santisteban *et al*. (2006) [17].

The practical example of the residual strain test at ENGIN-X neutron diffraction instrument at room temperature and unloaded condition presented here is for air plasma sprayed (APS) Mo-Mo_2C/Al_2O_3 coatings on to Hastelloy-X® substrate [5]. An example of a diffraction peak (scattered by polycrystalline materials [5, 22]) from a monochromatic instrument is shown in **Fig. 4**. Time-of-flight (TOF) diffractometers are typically used at pulsed sources (e.g. at ENGIN-X), where each pulse provides a diffraction profile across a large range of lattice spacings. The ENGIN-X instrument has a large flight path from the source to the sample (50 m) providing good $\frac{\Delta d}{d_{hkl}^0} = 50\mu\varepsilon$ resolution [17-18].

5. Test preparation

Electronic copy available at: https://ssrn.com/abstract=3711244

Before carrying neutron strain measurements at ENGIN-X, the preparation involves several steps, as careful planning as possible can help to minimize the losses of beamtime hours or days involved. These include preparation in view of understanding the coating and substrate crystal structure, planning neutron scanning, gauge volume and calibration of the instrument.

5.1 Microstructure assessment and plan for neutron scanning

Apart from size and shape of the specimen, it is important to know the material properties and microstructure before neutron scanning using some analytical instruments, such as X-ray diffraction (XRD) for phase analysis, energy dispersive spectroscopy (EDS) for elemental analysis and scanning electron microscopy (SEM) for microstructure analysis. These can be necessary as the thermally sprayed coating is composed of many crystalline and amorphous structure, and crystalline structures (to be analysed using neutron diffraction) may not be aligned with each other. The XRD analysis for material phases and for crystallographic planes of samples (coating and substrate part) can be very useful in identifying neutron spectra peaks at the ENGIN-X during experimentation. It is important to note that Miller indices for crystallographic planes have notations (hkl), and Miller index is defined as reciprocals of the fractional intercepts that the plane makes with the x-, y- and z-axes of the three non-parallel edges of the cubic unit cell. Interplanar spacing between two closest parallel planes with the same Miller indices is designated d_{hkl} [18]. The XRD of the coated surface can show the presence of the dominant phase. If there are distinct textural effects within the microstructure, the infinite orientations criterion of powder diffraction may not be met; in such cases, the some of the diffraction peaks might be missing completely and so may not match the reference peaks [5]. However, all major peaks can be identified using the International Centre for Diffraction Data (ICDD) software Powder Diffraction File™ (PDF) [23] numbers in the analysis.

Microstructure analysis using SEM for both coating surface and cross-section helps to identify the splat orientation or crack and residual defect within the coating layer, including any prior delamination of the coating at the interface. Some understanding of these features (coating layer) and comparison of associated residual strain measurement at ENGIN-X facility may help plan the full experiment with confidence [2-3]. The cross-sectional analysis may also provide exact coating thickness and information about bonding quality between coating and substrate at the interface. If the coating layer has a significantly high number of vertical cracks with layered pores (e.g. normally observed in some YSZ thermal barrier coatings [24]) or the bonding quality between coating and substrate at the interface has already been compromised

Electronic copy available at: https://ssrn.com/abstract=3711244

(i.e. delamination leading to stress relaxation), the residual strain measurement values may not be a true representation of the as-coated and as-received sample.

5.2 Sample gauge volume and counting times

Two important practical considerations are the gauge volume and the counting time for a given sample. How small should be the sample gauge volume for coating part, especially when the coating thickness is typically about 50 μm to 500 μm? This is the volume defined as a cuboid of sides ($\Delta V = \Delta x.\Delta y.\Delta z$). In neutron strain experiments, the diffracted signal is obtained from a defined volume [25] in space that contains part of the specimen material. Typically, some understanding of the structure and size of original sprayed powder (e.g. conventional, nanostructured) and through-thickness splat size can help define the gauge volume. The simplified sketch in **Fig. 5** presents how a sampling volume is defined through apertures (e.g. slits) placed in the incident and diffracted beams. The intersection of the incident and diffracted beams defined by slits and collimators defines the gauge volume [17]. Usually, the largest gauge volume can minimise the counting times (useful for bulk or large volume of material testing). However, different coating and substrate materials will require different counting times depending on the sample geometry, dimensions, and measurement point positions due to the neutron path lengths. Larger gauge volumes can be used to reduce counting times, but it needs to be optimised between counting time and measurement spatial resolution. The diffracted signal recorded on the detector (e.g. at Bank 1, Bank 2; centred at ±90° to the incident beam) in neutron strain and stress measurements originates from this volume [3]. In thermally sprayed coating sample testing, the gauge volume can be rastered across the sample through thickness (or vertical scan mode [2-5]), e.g. **Fig. 6(a,b)**, as the divergence perpendicular to the diffraction plane, does not affect the resolution. ENGIN-X uses a few sets of removable radial collimators, such as 0.5 mm, 1 mm, 2 mm, 3 mm, and 4 mm gauge width [7].

As demonstrated in previous work [5, 22], the scattering trials can be conducted in a vertical scan mode with a slit gap of 200 μm (or 0.2 mm, **see Fig. 7(c)**) to determine the through-thickness residual strain profile of the coating-substrate system. To achieve a high-resolution profile of the through thickness strain, a submerged beam near the coating surface can be used. The same can be done with the coating and substrate near the interface. As an example, a gauge volume of 0.2 mm × 8 mm × 4 mm can be employed. The 0.2 mm gauge size was defined along with the coating build-up direction necessary to maintain sufficient spatial resolution. The other dimensions can be increased up to 8 mm x 4 mm in the regions or directions where there are small strain gradients and minimal microstructure variations to minimise counting times. This

Electronic copy available at: https://ssrn.com/abstract=3711244

is necessary to ensure that the data point collection strategy is optimised for the beam time available.

Strain checks can be executed at the geometric centre of the specimen. To overcome the generation of pseudo-strains as the gauge volume moves out of the surface, it has been argued that the incident beam be scanned vertically out of a horizontal surface, as there would not be any change in the diffraction angle.[6]. The specimen position can be adjusted through the use of three orthogonal motors along the three co-ordinate axis (X,Y – Horizontal, Z – Vertical). The specimens can be moved along the Z-axis along steps of 50μm within the coating and in steps of 25μm within the substrate material (i.e. closer to the interface). A beam height of 0.2mm can be achieved by passing the beam through an assembly of horizontal and vertical slits. Partially submerging the gauge volume allowed the strain in the coated material with coating thickness 250 μm (**Fig. 6(b)**), whereas, a fully submerged beam can be used t measure the substrate strain. To measure the strain within the coating and substrate, different measurement times will be necessary (3 to 4 hours per vertical step along coating depth and coating-substrate interface), and fully in substrate (30-45 minutes per vertical step along substrate depth) [2-6].

5.3 Calibration of a neutron diffractometer

The calibration of the neutron diffractometer and associated instruments must be tested prior to scanning (normally carried by instrument scientist) using the procedure that has been verified according to practices at ENGIN-X. A sample configuration that produces statistically determinate strain in the sample must be used. The procedure must be repeated to ensure reproducibility of the measurement data and the repeatability must be examined. Calibration of the ENGIN-X neutron diffraction instrument is done through the determination of the wavelength of the incident neutron beam and the angular response of the neutron detector accurately [18]. At a TOF (e.g. ENGIN-X) source, isotropic neutron scatterers (e.g. vanadium) with very weak or no diffraction peaks of their own are used to perform the necessary calibration of the detector efficiency as a function of wavelength. [26].

6. Strain testing

Strain testing includes experiment preparation in view of sample mounting, reference point, fast scanning, full scanning of sample, and scanning for d_0-spacing (d_{hkl}^0).

6.1 Sample mounting

Sample positioning on stage is an important element of neutron diffraction strain measurement. In thermally sprayed coating sample investigations, the objective could

Electronic copy available at: https://ssrn.com/abstract=3711244

be to measure the distribution of strains through-thickness within the specimen (**Fig. 6(b)**), however, there could be other analysis as well. Hence, a sample positioning on stage should enable the change of location of the gauge volume within the sample. In some cases, a dedicated sample holder for mounting on the table may be needed, and this should be designed and built in advance in discussion with instrument scientist before visiting the ENGIN-X lab for experiments. As shown in **Fig. 7**, the ENGIN-X positioner where samples are mounted is a high capacity translation and rotation stage for 1-tonne maximum specimen weight (horizontal motion: ±250 mm, vertical motion: 600 mm, rotational about a vertical axis: 370°). Samples can be mounted with reproducible positioning on these breadboards using a LOCOMETRIC Precision Sample Mounting System [27]. If the experiment requires testing at a given temperature and external mechanical loading conditions, the servo-hydraulic stress rig and environmental test chamber (e.g. furnace or cryogenic, which can be varied at different rates) within the normal atmosphere or under inert gas, can be useful. The test samples could be mounted in loading fixtures (with a pre-stress) for sequential loading through a range of force and temperature as mentioned above. The change in interplanar d-spacing can then be measured for each force and temperature conditions [1, 26].

6.2 Reference point and fast scanning

These are a time-consuming but important step for the strain measurements. It is good practice to position the centroid of the gauge volume at the reference point. The ENGIN-X instrument reference axis and neutron beam reference height must be aligned at the centre of the instrument gauge volume (IGV) [18]. This is to refer to the position of the test sample. One practical method is to first centre a vertical pin on the table (ENGIN-X positioner, top tier) so that pin tip defines the reference point. The centring of the pin tip can be done by viewing the tip through a theodolite, which is an optical apparatus for measuring coordinates of visible points. The centring of the pin tip can also be done by using a micrometre contact gauge and adjusting the position of the translator. Following the centring steps, the gauge volume is arranged to have the reference point as its centre by positioning the apertures in the horizontal and vertical planes [18]. Once the sample has been mounted on the stage or table (ENGIN-X positioner, top tier), the necessary step in performing neutron diffraction of the effective position in the sample at which the strain is measured is important. This is typically done through fast scanning (using vertical scan mode, through-thickness of the coated sample) of thermally sprayed coatings (e.g. **Fig. 8**). The registration of diffracted neutron spectra, both at the start and end of the scan where scattering volume is partially filled, can give an abnormal peak shift which can be incorrectly interpreted as strain. These steps (reference point, fast scanning) can be adjusted to ensure that the centre of the neutron spectra intensity

Electronic copy available at: https://ssrn.com/abstract=3711244

profile versus the vertical position of the translator is in the encoder values corresponding to the reference axis position [18].

6.3 Scanning of coated sample for d-spacing

The experiments are typically conducted in vertical scan mode (**Fig. 6**) to measure the through-thickness residual strain profile of the coating-substrate system. Several samples can be assembled on a holder as shown in **Fig. 9(a)**. The details of the vertical scan method are described elsewhere for thermal spray coatings [2-6]. Strain measurements are typically performed at the centre of the specimen (at p_1) but can be performed at other locations as well (e.g. at a radial distance, r = 5 mm (at p_2) from the centre [3]), as shown schematically in **Fig. 5(c)**. Although the measurement locations in the specimen can be changed, the distance to the detectors (Bank 1 and Bank 2) is always the same. A partially submerged beam can be used at the coating surface and a beam submerged partially in the coating and the substrate can be used at the coating-substrate interface to obtain a high resolution profile of the through thickness residual stress distribution. Measurement of the residual strain at a volume smaller than the gauge volume using a partially submerged beam can be understood from other studies [17]. The coating-surface interface and the coating surface can be located within a resolution of 50μm with the help of fast vertical scans and careful location of the specimen using theolodites.

6.4 Scanning of materials for d_0-spacing

Though there is not a requirement to measure the stress free lattice spacing [18], the either removing the coating from the substrate and crushing to create the coating powder or direct measurement of the feedstock powder can be carried out to measure the strain-free lattice parameter (d_{hkl}^0) [2-6], as shown in **Fig. 9(b)**. This powder can then be put in a vanadium tube and its lattice parameter measured, as shown in **Fig. 9(c)**. The strain-free lattice parameter for the substrate can be measured at the suitable area of the uncoated substrate sample where d_{hkl}^0 has been verified to be independent of position and direction at that region in the materials [18] (or unsprayed substrate can also be used). In case dedicated reference samples are needed; these should be prepared in advance before visiting ENGIN-X lab for experiments or while other measurements are ongoing.

7. Strain and stress analysis

7.1 Pre-processing steps

Neutron spectrum are characterised by several parameters that can be analysed, e.g. position/shape/amplitude/width of the peak in the spectra, however, the positions and

Electronic copy available at: https://ssrn.com/abstract=3711244

widths of the spectra are important parameters which can be related to the strain field in the sample [18]. Typical steps after neutron diffraction testing of coated samples include plotting spectra (neutron counts v/s d-spacing; neutron counts v/s TOF; e.g. **Fig. 4,** and as an example, a set of experimental data and analysis is provided in **Appendix A,** using ISIS ENGIN-X software Open genie) for both banks (detectors) for each location. It is highly recommended to carry few preliminary analyses as soon the first few neutron spectra data is available during the experimentation. This can assist in the identification of neutron spectra peaks (corresponding to each hkl planes known, or identified through X-ray diffraction carried for test preparation) in both banks, and in locating depth where they had no or minimal overlap with other peaks. If one single or several non-overlapping peaks are measured, their spectra parameters are analysed for each peak separately, however, the analysis of the whole spectrum can be performed using Rietveld methods.

7.2 Post-processing steps

The post-processing steps include a listing (normally MS Excel spreadsheet used; as an example, a set of open access experimental data and analysis is provided in **Appendix A** (for RB1510238 [22]) of $d_{hkl}$and d_{hkl}^{0} spacing for each run number and bank number (both in coating and substrate part) in a sample. The analysis of $d_{hkl}$and d_{hkl}^{0} spacing in diffraction peaks for the coating and substrate materials is possible either (or both) using the Rietveld refinement method or individual peak method. Use of the Rietveld refinement method may be easy, however, in the individual peak method, the listing of d_{hkl} and d_{hkl}^{0} spacing needs to be done for each identified peak for peak-by-peak analysis. The peak-by-peak analysis can help in analysing the strain for each *hkl* planes.

Evaluation of the lattice parameters in the case of simple crystal structures can be carried out through the Rietveld refinement analysis which considers multiple peaks in the spectra. However, where the spectra has overlapping peaks, e.g. coating to substrate and substrate to coating, this method can be challenging to apply. . At each measurement location, the neutron spectra recorded by the individual detectors are time focused using the computer code GSAS [28]. Using a library of common engineering materials, this software automatically refines the single-peak and full-spectra within the diffraction spectra [17]. To ensure the convergence of the refinement, single-peak refinement of the most intense peak is performed to speculate the lattice parameters initially.

7.3 Strain calculations

7.3.1 Rietveld profile refinement

Electronic copy available at: https://ssrn.com/abstract=3711244

The standard method of analysing the neutron diffraction experimental results is the Rietveld profile refinement method. In this, the intensity measured as a function of the scattering angle is fit with the parameters of a model. The strain can be obtained from the shift in diffraction peaks for the coating and substrate materials using Rietveld refinement. The Rietveld method allows analysis of spectra with strongly overlapping lines and patterns from multiphase materials. A change in in d-spacing or $\Delta d = (d_{hkl} - d_{hkl}^0)$ in the lattice spacing due to internal strains will result in a shift of a Bragg peak position $\Delta\theta$ (typically in the range of 0.005° to 0.2°) when a single wavelength is used [18]. The General Structure Analysis System (GSAS) software [28] can be used in the data analysis. The fitting parameters of the refinement, confirming good fit to the diffracting pattern.

7.3.2 Individual peak fitting

The strain can also be obtained from the shift in 'individual' diffraction peaks for the coating and substrate materials using a single peak fitting routine [21] using GSAS software. The fitting parameters of the refinement, confirming good fit to the diffracting pattern (shown in **Fig. 4(b)**). The peaks chosen for the strain analysis should be such that they had no or minimal overlap with other peaks. As an example, a set of experimental data and analysis is provided in **Appendix A** (for RB1510238 [5, 22]).

7.3.3 Strain calculations

After analysing individual diffraction peaks results, residual strain ($\varepsilon_{hkl} = \frac{d_{hkl} - d_{hkl}^0}{d_{hkl}^0}$) results in coatings and substrate can be analysed using individual peak method or Rietveld (using Equation 5). **Figure 10** shows an example of residual strain measurement (plotted using single peak fitting routine analysis). The averaging of strain across the various identified crystallographic planes can also give similar results to the Rietveld refinement.

7.3.4 Stress calculations

The average coating and substrate residual strain (and stress) can vary significantly with the coating conditions. From the measured strain, the residual stresses can be determined using the elastic constant (Hooke's law, Equation 6) for material types, where bulk elastic modulus values of materials are typically used from literature or through standard mechanical testing of samples (e.g. bending/tensile tests). However, as shown in **Fig. 11(a)**, number of nanoindentation based elastic modulus measurement for stress measurement ($\sigma = \varepsilon E$) can be done on each coating-substrate cross-section, which can be dispersed in five lines of 5 measurement points each, at a specific space from the boundary (i.e. coating surface). Indentations can be spaced by several microns

Electronic copy available at: https://ssrn.com/abstract=3711244

apart, to avoid any interaction of adjacent indentations. By the same method, some 10 measurements can be spread in two lines of 5 measurement points apiece on each substrate cross-section near the interface, at a specific distance from the interface. To convert the through-thickness residual strain data to analyse the corresponding residual stress distribution, an average value of measured elastic modulus can be utilized where the measurement depth location of residual strain and elastic modulus did not match. As an example, a set of experimental data and analysis is provided in **Fig. 11(b)**, and analysis is provided in **Appendix A**.

If required, the stresses can then be normalised by dividing by the yield stress data ($\frac{\sigma}{\sigma_y}$) of the coating and substrate materials, respectively. In the example shown (**Fig. 12**), the yield stress of the Hastelloy-X® substrate is taken as 385 MPa and for Mo-Mo_2C/Al_2O_3 it is taken as 770 MPa (at zero plastic strain) [30]. As shown, both for coating and substrate parts, the normalised stress $\frac{\sigma}{\sigma_y} < 1$.

7.3.5 Precision and bias

Neutron scattering allows the atomic positions in the structure to be determined with high precision. At ENGIN-X, the precision of neutron diffraction instrument alignment within 50 με can be achieved [17]. The accuracy of this method is considered to be absolute, however, the error or uncertainties can be related to various factors, such as quality of the diffracted neutron peaks (background, noise), calibration, failure to consider appropriate time during the measurement to obtain accurate scattering intensity and the peak positions. Other factors could be variation in temperature or chemical composition of the sample as a function of position and time, including measurements if performed in regions with steep strain gradients [18] (e.g. coating-substrate interface) can also add to error, leading to uncertainty in strain.

8. Examples of neutron diffraction of thermal spray coatings at other facilities worldwide

Neutron sources worldwide (e.g. Africa, Asia, Australia, Europe, and North America) have been used to test strains (and stress) in various materials. Overall, there are two types of stress diffractometers ((a) monochromatic, where diffraction pattern is a function of the scattering angle, and (b) time-of-flight (TOF) or continuous incident spectrum, where the diffraction pattern is a function of time-of-flight [18]). There are not many but good number of examples where thermal spray coatings have been characterised to study strains as well as microstructures (e.g. porosities, volumetric and size characterization of void morphologies, texture) using neutron diffraction techniques. As described above, the ISIS/ENGIN-X neutron facility have been used to measure residual strain in thermal

Electronic copy available at: https://ssrn.com/abstract=3711244

spray coatings [2-6] and [9-13], the methodology of which has been summarised in practical steps summarised above. This section presents some examples, however, by no means presents a comprehensive critical review on the application of neutron scattering techniques to study thermal spray coatings, at laboratories worldwide (such as NECSA/MPISI, ANSTO/KOWARI, NIST/BT8, ILL/SALSA, LLB/DIANE, HZB/E3, GEMS/STRESS-SPEC, PSI/POLDI, BARC/SANS, ANSTO/ECHIDNA, ILL/D20, NIST/SANS, ORNL/HB-2B, and LANSCE/HIPPO).

8.1 Strain analysis

As will be seen through examples below, KOWARI instrument at ANSTO in partnership with other neutron sources (e.g. BT8 instrument at NIST, MPISI instrument at NECSA), have been regularly used to study residual strains in thermally sprayed and cold sprayed coatings. For coated samples of various thicknesses, investigators have used various gauge volumes with slit widths (0.2 mm, 0.3 mm, 0.5 mm) in through thickness dimension. Interestingly, different strategies were considered to obtain strain-free lattice parameter (d_{hkl}^{0}) for the coating and substrate part. However, to measure residual strains (and stresses) averaged over gauge volume, d_{hkl} (in-plane component) and d_{hkl} (normal-plane component) values were used mainly, using an equal-biaxial stress approach, and implementation of elastic constant (Hooke's law) [31-32].

Using MPISI instrument at NECSA and KOWARI instrument at ANSTO, Venter et al. [33] studied 200 μm thick HVOF sprayed coatings (e.g. WC-12wt%Co, WC-10wt%VC-12wt%Co) deposited on to 4 mm thick mild steel substrate. The residual strains were investigated in the erosion wear scar regions. While using the test protocols of MPISI instrument [34], the focus was to study the strain behaviours in the substrates by employing through-thickness fine measurement, and by doing so, the stress in the coating could be determined by imposing strain balance in the sample. While using the test protocols of KOWARI instrument [35], with diffracted beam slit at a width of 0.3 mm, and positioning the gauge volume in the centre of the 200 μm thick coating, the strains were measured directly in the coatings [33]. It was proposed that it is almost impossible to provide unstressed reference material (due to thin layer of coatings) and used equal-biaxial stress approach. Overall, the neutron scattering results indicated that the erosion impact angles influenced the residual strains and the coating composition.

Using KOWARI instrument at ANSTO, Luzin et al. [36] studied through thickness residual stresses in three coating materials sprayed using HVOF (JP 5000, DJ2700). The samples included: (a) 0.5 mm thick Ni coating on AISI 1008 carbon steel substrate (2.6 mm thick plate) was deposited using JP 5000 (Praxair TAFA), (b) 0.25 mm thick Ni-29%Cr coating on low carbon steel substrate (1.64 mm thick plate) was deposited using DJ2700 (Diamond Jet gun) and (c) 0.25 mm thick WC-17%Co coating on ferritic and

Electronic copy available at: https://ssrn.com/abstract=3711244

austenitic steel substrates (2.2 mm thick plate) was deposited using JP 5000 (Praxair TAFA). A gauge volume 0.2 x 0.2 x 15 mm^3 (as well as 0.3 mm) in the through thickness dimension was used and applied equal-biaxial stress approach to obtain residual stresses. In the examples shown, it was observed that the method was capable for stress characterisation in coatings with thickness ranging from 0.2 mm to many millimetres, and through-thickness resolution of 0.2 mm can be useful for routine and serial measurements in various coating substrate systems, potentially enabling optimisation of spray process parameters.

Using KOWARI instrument at ANSTO, Oladijo et al. [37-38] studied through thickness residual stresses in HVOF sprayed 250 μm to 500 μm thick Inconel 625 coating on 304 stainless steel substrates of 3 mm thickness. A gauge volume 0.2 x 0.2 x 20 mm^3 in the through thickness dimension was used and applied equal-biaxial stress approach to obtain residual stresses. It was observed that the residual stressed were compressive in nature (approximately same for all samples), and the residual stresses increased slightly with increased coating thickness.

Using KOWARI instrument at ANSTO, Smith et al. [39] studied through thickness residual stresses in HVOF sprayed 365 μm thick Ni-914-3 deposited on two different substrate geometries. The two geometries were cylindrical hourglass (cold-drawn 1018 steel, 12.7 mm diameter and 101.6 mm length), and flat beams (machined and heat-treated 1008 mild-steel, 228.6 x 25.4 x 2.38 mm). Residual strain measurements were performed with a gauge volume of 0.2 x 0.2 x 20 mm^3, with the elongated gauge volume (oriented parallel to the in-plane direction and crack interface). Interestingly, stresses were measured in the three principal directions (i.e. two in-plane and one normal to the coating surface). Residual strain in substrate only (i.e. without coating) was also measured using the same method to address possible pre-coating stress within the substrate. The stress profiles were then subtracted from the stress profiles of the coated samples so that the reported stress profiles are only associated with the spraying process only. Two methods for the residual stress measurement were used (i.e. before and after subjection of coated samples to a partial loading regime via cantilever bend fatigue). It was observed that the distribution of the residual stresses within a coating-substrate system can be influenced by the application of external mechanical loading stresses into the system. The effect of increased compressive residual stress within the coating surface during cantilever fatigue loading was also observed, due to the geometry and test configurations.

Using KOWARI instrument at ANSTO, Saleh, Luzin and Spencer [40] studied through thickness residual stresses in two coating materials sprayed using cold spray techniques (i.e. kinetic metallization or low-pressure cold spray, and supersonic cold spray). The samples included 3-4 mm thick AA-6061-T6 cold spray coatings on Al and

Electronic copy available at: https://ssrn.com/abstract=3711244

Mg substrates (each 3 mm thick). Residual strain measurements were performed with a gauge volume of 0.5 x 0.5 x 18 mm^3. Stresses were measured in the two principal directions (i.e. in-plane and one normal to the coating surface) and applied equal-biaxial stress approach to obtain residual stresses. Residual strain in substrate only (i.e. without coating) was also measured using the same method to address possible pre-coating stress within the substrate. The stress profiles were then subtracted from the stress profiles of the coated samples so that the reported stress profiles are only associated with the spraying process only. It was observed that the Al coating is in slight compression, and regardless of the substrate material, the two Al coating stress profiles were similar, because of similarity in thermal and mechanical properties of Al and Mg.

Using KOWARI instrument at ANSTO, Luzin et al. [41] studied through thickness residual stresses in cold sprayed additively manufactured (CSAM), a thick patch coated sample produced from titanium powder. The coating of thickness 3.2 mm was deposited on 6.2 mm thick stainless steel substrate of size 30 mm x 30 mm, whereas the long bar of cross-section 5.2 mm thickness and 3.44 mm width was sprayed on Al substrate (66 mm x 66 mm 2.8 mm). For coating sample, residual strain measurements were performed with a gauge volume of 0.5 x 0.5 x 20 mm^3. Stresses in coating was measured in the three principal directions (i.e. two in-plane and one normal to the coating surface). Residual strain in substrate only (i.e. without coating) was also measured using the same method to address possible pre-coating stress within the substrate. The stress profiles were then subtracted from the stress profiles of the coated samples so that the reported stress profiles are only associated with the spraying process only. For bar sample, residual strain measurements were performed with a gauge volume of 1 x 1 x 1 mm^3. The three principal stress components can be calculated using the measurements taken from the three principal directions with the constant d_{hkl}^0. Isotropic elastic diffraction constants were used to calculate the stresses from the measured strains. From analysis, it was observed that in both sample types the residual stress was mainly formed through thermal mismatch mechanism, due to the coefficient of thermal expansion (CTE) difference between substrate and deposited coating. The overall results also demonstrate the dependence of the stress state on the sample geometry. A change in the sample geometry leads to the stress being measured change from a biaxial state to a uniaxial state.

Using KOWARI instrument at ANSTO, Kim et al. [42] studied the effect of low temperature range heat treatments (100-400 °C) on the residual stress of cold sprayed Inconel®718 coating of 1.1-1.4 mm thickness deposited onto a presolution-treated Al7075-T651 substrate (305 mm x 305 mm x 24 mm). Residual strain measurements were performed with a gauge volume of 0.3 x 0.3 x 20 mm^3. Stresses were measured in the two principal directions (i.e. one in-plane and one normal to the coating surface).

Electronic copy available at: https://ssrn.com/abstract=3711244

The coating was assumed to be in a bi-axial stress state with the stress in the direction normal to the surface assumed to be zero for thin coatings. Kim et al. [42] suggested that the existence of zero stress condition in the direction normal to the thickness is a valid assumption for the coating with the thickness of up to 2mm but not for the substrate with much higher thickness. This assumption is still valid for the substrate till a distance of 2mm from the interface. The effect of the heat treatment temperature on the stress relaxation was also demonstrated. Lower temperature helped relieve the stresses whereas a higher temperature resulted in a residual compressive stress in the Inconel 718 coating and a residual tensile stress in the substrate.

Using the test protocols of STRESS-SPEC@FRM II instrument at GEMS, Gibmeier et al. [43] studied local phase and residual strains for yttria stabilised zirconia (YSZ) thermal barrier coatings (TBC). The coatings were deposited using a mix of techniques (air plasma spray/APS; high velocity oxy-fuel/HVOF; vacuum plasma spray/VPS) on two different substrates (Inconel IN 738 LC, nickel-based superalloy/Mar M 247; 32 mm diameter and 3 mm thick). After coating, the samples were subjected to cyclic and isothermal heat treatments. Through surface strain scanning was carried for local residual stress analysis to analyse diffraction data from all contributing layers (i.e. topcoat: 8-wt% Y_2O_3 stabilized ZrO_2 with thicknesses 360 µm to 671 µm; bond coat: Amdry 386 or NiCoCrAlY-alloy with thicknesses 205 µm to 230 µm) and of the substrate material. However, to measure residual strains, d_{hkl} (heat-treated) was compared to d_{hkl}^{0} (as-sprayed). It was proposed that it is almost impossible to provide unstressed reference material (due to thin layer of coatings) with identical microstructure to determine stress-free d_{hkl}^{0}. From the measured strain, the residual stresses were determined using the elastic constant (Hooke's law) for material types determined based on bending experiments. The heat treatment led to the YSZ topcoat exhibiting a compressive residual stress in the in-plane and out-of-plane direction. Whereas in the bond coat a tensile residual stress was seen for the reason of balancing the stress. Compared to isothermal loading, cycling thermal loading led to a higher degree of compressive residual stresses towards the surface of the YSZ topcoat. Similarly, the degree of tensile loading within the bond coat increased with cyclic thermal loading.

Using HMI instrument at HZB and SALSA instrument at ILL, Lyphout [44] investigated residual strains in HVOF sprayed Inconel 718 coatings (four different thicknesses: 1, 1.5, 2, 2.5 mm) on Inconel 718 substrates (25.4 mm diameter and 3 mm thickness). In their experiments, a freestanding coating and an annealed grit blasted substrate respectively to balance the stress to obtain the d_{hkl}^{0} value. Reflection and transmission modes were used can the sample from top to bottom to calculate the radial and axial stresses. From the measured strain, the residual stresses were determined using the elastic constant (Hooke's law) for material types. Increasing the

Electronic copy available at: https://ssrn.com/abstract=3711244

coating thickness (i.e. 1 mm to 2.5 mm) did not modify through-thickness residual stress in coatings, and overall compressive stress was achieved both in coating and substrate at the interface, but the difference in stress amplitude at the interface seems to significantly decrease when coating thickness was increased.

Using POLDI instrument at SINQ, Kovářík et al. [45] investigated plasma sprayed Ni10wt%Al (about 100 μm thick) and Cr_2O_3 (about 150 μm thick) onto mild steel (S235JRC, 4 mm thickness) substrate. Through thickness, residual strain profile (slightly below the substrate surface) was measured in the mild steel substrate only due to very low diffracted signal in coatings part. Strain-free lattice spacing (d_{hkl}^0) was determined from the measurement at the centre of the coated specimen. From the measured strain, the residual stresses were determined using the elastic constant (Hooke's law) for material types (analysed by selecting the most intense peak of the spectra). In the example shown, it was observed that the compressive residual stress (originated by grit blasting and preserved below the Cr_2O_3 layer) was present close to the substrate surface, and the maximum value of compressive stress was measured in the coating combination (i.e. Ni10wt%Al on Cr_2O_3 specimen).

Using the BT8 instrument at NIST, Luzin et al. [46] investigated various thermally sprayed coatings ranging from thick deposits (about 10–30 mm thick) to less than 500 μm thick coatings. The coatings included cold sprayed Al powder on Al substrate, plasma sprayed Si powder on Cu substrate, HVOF and plasma sprayed Mo_2C-Mo powder on steel substrate and iron sample by spray forming. They implemented different residual stress measurement strategy for coatings of different thicknesses. For example, for thin coatings, (<0.5mm), an average through thickness stress value was calculated along with a normal and in-plane stress to resolve the in-plane stress and the stress-free d-spacing (d_{hkl}^0). For medium thickness coating (0.5<t<5 mm), the assumption of zero normal stress was approximated, however, the through-thickness measurement was possible, including two measurements per measurement point were suggested to be sufficient. For thick coating (t>5 mm), the assumption of normal stress (to be zero) was suggested. For thick coating, to resolve the three principal stress components, the knowledge of atleast three independent measurements and the stress free spacing (d_{hkl}^0) is required. It was proposed that owing to their high penetration, neutrons allows stress profiling through the coating thickness, and multiphase materials can be studied, including the effect of other surface treatments, such as shot peening, and laser peening.

Using BT8 instrument at NIST, Li et al. [47] investigated residual strains of single splats as well as 380 μm thick coatings of plasma sprayed molybdenum deposited onto 1040 steel (2.4 mm thick). From the measured strain, the residual stresses were determined using the elastic constant (Hooke's law) for material types (analysed by

Electronic copy available at: https://ssrn.com/abstract=3711244

selecting the most intense peak of the spectra). Though no apparent residual stress was found in the 380 μm coating, a single splat layer exhibited a high residual stress due to the high degree of bonding of the first splat layer and stress relaxation within the coating due to the large number of defects.

Using the BT8 instrument at NIST, Luzin et al. [48] in continuation of Choi et al. [31] work related to cold spray Al coatings, investigated surface and in-plane stresses in Cu and Al cold sprayed coatings. Cold sprayed Cu (onto Cu and Al substrates) and Al (onto Cu and Al substrates) samples were about 3 mm thick. The Cu substrates were 3.1 mm thick, whereas the Al substrates were 2.6 mm thick [48]. A gauge volume 0.5 x 0.5 x 18 mm^3 was used. The internal stress in the freestanding substrates were measured before the cold spraying, and this internal stress was subtracted to isolate stresses induced by the cold spray process. From the measured strain, the residual stresses were determined using the using the assumption of a balanced biaxial plane stress state [31]. It was observed that the kinetic parameters of the cold spray process, the deformation behaviour of the particles and the feedstock material properties dictate the residual stress within the coating [48]. Compared to Al coatings, the mechanical properties of the Cu coating were closer to bulk properties. The higher plastic strain the Cu coatings resulted in higher residual stress in the Cu coatings and higher compaction [48].

Using the BT8 instrument at NIST, Luzin et al. [32] investigated residual stresses in low-pressure cold sprayed coatings (e.g. Al-Al_2O_3 metal matrix composite) of 1 mm thickness onto 3 mm thick A16061 aluminium substrate. A gauge volume 0.5 x 0.5 x 20 mm^3 was used and applied equal-biaxial stress approach to obtain residual stresses. In the example shown, it was observed that the overall residual stress in the coating was compressive. Also, due to the elevated spray temperature characteristic of low-pressure cold sprayed coatings (dynamic metallization), thermal stresses were also present, and because of the multi-phase composition and thermal mismatch between the metal and ceramic components of the metal matrix composite (MMCs), inter-phase micro-stresses also accumulated, leading to overall compressive residual stresses [32].

Using DIANE instrument at LLB, Ceretti et al. [49] investigated residual strain profile from the coating surface to the material through the interface in a ferritic steel cylinder having 78 mm diameter. The elastic constant (Hooke's law) related to the most intense peak of the spectra were measured with respect to the three principal directions.

8.2 Other analysis

Small-angle neutron scattering (SANS) techniques [50] helps analyse the total specific surface area of the voids (size up to about 100 nm), whereas, multiple small-angle neutron scattering (MSANS) technique can help analyse average pore size and orientational distribution. Using SANS and MSANS techniques at NIST, Keller et al. [51]

Electronic copy available at: https://ssrn.com/abstract=3711244

studied the void microstructures (i.e. interlamellar pores, intra-lamellar cracks, and volumetric globular voids, each having different volume fractions, anisotropy, size, and shape) of APS sprayed NiCrAlY coatings. Keller et al. [51] suggested that for the NiCrAlY coating, inter-lamellar cracks constituted only a small portion of the void fraction whereas the interlamellar pores were a major portion of the void system. Similarly, using SANS technique at BARC, Sen et al. [52] investigated evolution of pore morphology during initial and intermediate stages of sintering in ZrO_2–3 mol% Y_2O_3. The analysis indicated a monotonic reduction in the net porosity with a growth in the net pore size during the initial and intermediate stages of sintering. Pore size growth was reported to an indirect consequence of the small pore coalescence due to the reorientation and grain mass transport during sintering.

The HIPPO instrument at LANSCE provides a range of material information including crystallographic textures, phase fractions, lattice parameters, and micro-strain. At HIPPO instrument, Takajo et al. [53] investigated crystallographic textures and phase fractions of involved phases of 23.8 μm to 34.0 μm thick Zr-coatings deposited on U-10Mo foils (0.3 mm thick). Texture, being responsible for the anisotropic physical properties of materials, reflects the thermomechanical history including recrystallisation, particle rotation and phase transformation. In addition, the bulk texture of a polycrystalline material constitutes the orientation distribution function of the crystallographic orientation with respect to the sample coordinate system [54]. The texture analysis of the coated surface showed [53] that selective grain growth likely caused considerable change in the texture at high temperatures. Also, Takajo et al. [53] suggested that Zr coating showed a preferential orientation and correlated with the initial texture of the uncoated U-10Mo.

Using D20 instrument at ILL, Jakani et al. [55] investigated crystallinity of plasma sprayed hydroxyapatite coatings (feedstock was micro and nano-sized particles) deposited onto a Ti-6Al-4V substrate. The sample was heat-treated (2 hours at 600 °C) to reduce amorphous fractions. Using the neutron spectra of samples (feedstock powder and coatings), Jakani et al. [55] observed that the deposited coating showed retention of the nano-meter crystallite and no secondary phases were identified. This meant that the nano-coating will have nucleation cites to the reconstituted bone, which will allow stabilisation of the implant in the bone.

Using HB-2B instrument at ORNL, Liu et al. [56] investigated the plastic deformation in a series of low-pressure cold sprayed Al-Cu coatings (on Al-Cu-Mg-Mn alloy (AA2024) substrate) using dislocation density as an indicator. for The copper content ranged from 2 mass% to 5 mass%. Analysing the neutron diffraction peaks, it was observed that the increase in the copper alloy additions (from 2 mass% to 5 mass%)increased the breadths of full width at half maximum (FWHM) of the cold

Electronic copy available at: https://ssrn.com/abstract=3711244

sprayed coatings increased, meaning the dislocation density in the Al-Cu coatings systematically increased with increasing Cu alloy content . Liu et al. [56] also showed that the peak breadth (FWHM) changes from the substrate to the coating and through the coating, and this change throughout the coating was accounted for by the fact that a the regions near the coating-substrate interface saw a larger number of repetitive impacts from subsequent particles than the rest of the areas towards the top surface of the coatings.

Using the powder diffractometer ECHIDNA at ANSTO OPAL (wavelength of 1.622 A°), Luzin et al. [48] investigated oxide volume fraction of Cu and Al feedstock powder materials for cold sprayed coatings. The analysis was carried to compare it against the feedstock powder, and to confirm the chemical purity of the feedstock powders. It was experienced that the usage of neutron powder diffractometer is better compared to X-ray diffraction, because the X-ray diffraction could only provide surface properties and not the subsurface, whereas the neutron diffractometer provides a better average measurement.

Table 1 summarise examples where thermal spray coatings have been characterised to study strains as well as microstructures.

Electronic copy available at: https://ssrn.com/abstract=3711244

Table 1. Neutron diffractometers for strain measurement and microstructure (with thermal spray coating examples only).

Institute	Facility & beam type [9]	Testing thermal spray coatings	Ref.
Africa			
South African Nuclear Energy Corporation SOC Limited (NECSA), South Africa	MPISI (monochromatic)	Strains	[33]
Asia			
JAEA Research Reactors, Tokai, Japan	TAKUMI (time of flight/TOF)	-	-
Hi-Flux Advanced Neutron Application Reactor (HANARO), Republic of Korea	RSI (monochromatic)	-	-
Bhabha Atomic Research Centre (BARC), Mumbai, India	PD-3 (monochromatic) SANS (monochromatic)	- Microstructures	- [52]
China Mianyang Research Reactor of China Academic of Engineering Physics (CAEP), China	RSND (monochromatic)	-	-
Badan Tenaga Nuklir Nasional (*BATAN*), Indonesia	DN1 (monochromatic)	-	-
Pakistan Institute of Nuclear Science and Technology (PINSTECH), Pakistan	Residual stress diffractometer (monochromatic)	-	-
Australia			
Australian Centre for Neutron Scattering (ACNS), ANSTO, Australia	KOWARI (monochromatic) ECHIDNA *(*monochromatic*)*	Strains Volume fraction	[31-33, 36-42]; [48]
Europe			
ISIS-Rutherford-Appleton Laboratories, UK	ENGIN-X (time of flight/TOF)	Strains	[2-6, 9-13, 57-59]
Institut Laue-Langevin (ILL), Grenoble, France	SALSA (monochromatic) D20 (monochromatic)	Strains Microstructures	[44] [55]
Laboratoire Léon Brillouin (LLB), Saclay, France	DIANE (monochromatic)	Strains	[49]
Helmholtz-Zentrum Berlin (HZB), Germany	E3 (monochromatic)	Strains	[44]
GEMS at Helmholtz-Zentrum Geesthacht, Germany	STRESS-SPEC (monochromatic)	Strains	[43]
Budapest Neutron Centre (BNC), Hungary	ATHOS (monochromatic)	-	-
Institute for Nuclear Research (INR), Romania	DIR 1 (monochromatic)	-	-
Joint Research Centre, Institute of Advanced Materials, Petten, The Netherlands	HB4 & HB5 (monochromatic)	-	-
SINQ, Paul Scherrer Institut (PSI), Switzerland	POLDI (time of flight/TOF)	Strains	[45]
Frank Laboratory of Neutron Physics (FLNP), Dubna, Russia	EPSILON-MDS and SKAT, FSD (time of flight/TOF)	-	-
St. Petersburg Neutron Physics Institute (PNPI), Gatchina, Russia	ARES (monochromatic)	-	-
Nuclear Physics Institute (NPI), Rez, Czech Republic	TSKN-400, HK4 (monochromatic)	-	-
North America			
NIST Center for Neutron Research (NCNR), US	BT8-DARTS (monochromatic) SANS 30 m NG3 (monochromatic)	Strains Microstructures	[31-32, 46-48]; [51]
Oak Ridge Neutron Facilities, US	VULCAN (time of flight/TOF) HB-2B NRSF (monochromatic)	- Microstructures	- [56]
Los Alamos Neutron Science Center (LANSCE), US	HIPPO (time of flight/TOF) SMARTS (time of flight/TOF)	Microstructures -	[53] -

Electronic copy available at: https://ssrn.com/abstract=3711244

9. Concluding remarks

In terms of residual strain measurement advancement, it has been argued that X-ray diffraction (synchrotron) non-destructive methods results in radiation that does not penetrate very well into the material subsurface layers and the substrate. However, in recent times neutron diffraction technique has been used on numerous thermal or cold spray coating materials to measure residual strains including microstructures. Likewise, neutron diffraction has been argued to be superior (but expensive and potentially time-consuming) for characterisation purposes especially in the characterisation of the structural evolution during heating, annealing, and cooling because of its high flux and deeper penetration of the neutron beam.

While applying neutron diffraction test protocols and implementing appropriate analysis strategies, from examples discussed in sections above, there are several studies where residual strains have been investigated for materials deposited through thermal or spray methods at neutron diffractometers mainly at ISIS/ENGIN-X, ANSTO/KOWARI and NIST/BT8, and some at NECSA/MPISI, ILL/SALSA, LLB/DIANE, HZB/E3, GEMS/STRESS-SPEC, and PSI/POLDI. Apart from residual strain analysis, microstructures of thermal or cold spray coatings have also been investigated at other neutron diffractometers (e.g. BARC/SANS, ANSTO/ECHIDNA, ILL/D20, NIST/SANS, ORNL/HB-2B, and LANSCE/HIPPO). Overall, for coated samples of various thicknesses, investigators have used various gauge volumes with slit widths (e.g. 0.2 mm, 0.3 mm, 0.5 mm) in through thickness dimension. Interestingly, different strategies were considered to obtain strain-free lattice parameter (d_{hkl}^{0}) for the coating and substrate part, and to measure residual strains (and stresses) averaged over gauge volume, d_{hkl} (in-plane component) and d_{hkl} (normal-plane component) values were used mainly, using an equal-biaxial stress approach, and implementation of elastic constant (Hooke's law).

Neutrons diffraction using ENGIN-X beamline (time-of-flight) is particularly useful at the coating-substrate interface as when the gauge volume is half/half in the coating-substrate system, one can identify both materials properties without losing any positioning accuracy in terms of the centre of gravity of the neutron beam. Additionally, in comparison to monochromatic sources where only single-phase materials can been investigated, easily on ENGIN-X (time-of-flight) dual phases (like duplex stainless steel) and multi-phase thermal spray materials can be successfully investigated.

Research in thermal spray area, however, does not comparatively evaluate destructive and non-destructive techniques to understand the through thickness residual stress within the coating-surface system. The cross correlation of the independent techniques is vital, as measured values of stress in the coating-substrate system can be sensitive to the stress measurement technique, which in turn influences the validation of

Electronic copy available at: https://ssrn.com/abstract=3711244

the numerical and mathematical methods of residual stress measurement and monitoring in coating systems.

Non-destructive measurement of these strain (or stress) fields in relatively thin thermal spray coatings also poses a challenge, as the conventional techniques such as laboratory X-ray, synchrotron X-ray and deep hole drilling are destructive in nature and are capable of only providing a sub-surface strain measurement. Surface roughness effects further complicate the very near-surface residual stress measurements which are important for near-surface crack initiation during wear. This drawback poses a challenge with residual stress measurement in thermal spray coatings as the through thickness stress measurement would require layer removal. There is also very limited literature that discuss correlations between strain measurement, structure-property relations and effect of post-treatment on the performance of such coatings which can result in harmonization of the strain field within the coating, and at the coating-substrate interface.

Other emerging challenges include testing new composite coating materials and new coating techniques applied (e.g. suspension or solution based thermal spray coatings manufacturing using nanostructured feedstock powders [e.g. 57-59]), including strain testing on actual coated parts of various geometries (e.g. curved, spherical, cylindrical, edges, corners, etc). Applicability of neutron diffractometers for residual strain and microstructure analysis could be a limiting factor for coating layers produced using nanostructured feedstock powders where small crystal size is still a bottleneck. There are other approaches and schemes for testing and predicting residual stresses in thermal spray coatings [60], however, issues regarding the accuracy, applicability, distribution analysis can be further looked into using principles of artificial intelligence (AI) and machine learning (ML) approaches [61-62].

Appendix A. Supplementary data

Supplementary data associated with this article can be found in the online version (open access), at https://doi.org/10.1007/s11340-017-0298-7 & https://data.isis.stfc.ac.uk/doi/INVESTIGATION/58451518/. Example steps to find d-spacing from neutron spectra and full data analysis can be found here.

- Finding d-spacing from neutron spectra
- Supplementary Data-RB1510238

Declaration of competing interest

The authors declare that they have no known competing financial interests or personal relationships that could have appeared to influence the work reported in this paper.

Electronic copy available at: https://ssrn.com/abstract=3711244

CRediT authorship contribution statement

Nadimul Faisal: Conceptualisation, Methodology, Testing, Analysis, Validation, Data curation, Writing - Original and final draft preparation, reviewing and editing. **Rehan Ahmed**: Conceptualisation, Methodology, Testing, Analysis, Validation, Writing - review & editing. **Anil Prathuru**: Experimental support, reviewing and editing. **Anna Paradowska:** Experimental support, reviewing and editing. **Tung-Lik Lee:** Experimental support, reviewing and editing.

Acknowledgements

The authors and instrument scientists acknowledge gaining neutron strain testing and analysis experience through several awards of ENGIN-X beamtime at the STFC ISIS facility for the neutron diffraction measurements of thermal spray coatings (e.g. RB1510238, RB910205, RB810413, RB15141, RB1120507, RB13990, RB38308).

References

[1] S. Y. Zhang, A. Evans, E. Eren, B. Chen, M. Pavier, Y. Wang, S. Pierret, R. Moat, B. Mori, ENGIN-X – instrument for materials science and engineering research, Neutron News, 24(3), 2013, 22-26.

[2] R. Ahmed, N. H. Faisal, A. M. Paradowska, M. Fitzpatrick, K. A. Khor, Neutron diffraction residual strain measurements in nanostructured hydroxyapatite coatings for orthopaedic implants, Journal of the Mechanical Behavior of Biomedical Materials, 4(8), 2011, 2043-2054.

[3] R. Ahmed, N. H. Faisal, A. M. Paradowska, M. Fitzpatrick, Residual strain and fracture response of Al2O3 coatings deposited via APS and HVOF techniques, Journal of Thermal Spray Technology, 21, 2012, 23-40.

[4] R. Ahmed, M. E. Fitzpatrick, N. H. Faisal, A comparison of neutron diffraction and hole-drilling residual strain measurements in thermally sprayed coatings, Surface and Coatings Technology, 206, 2012, 4180-4185.

[5] N. H. Faisal, R. Ahmed, A. K. Prathuru, S. P. Katikaneni, M. F. A. Goosen, Shu-Yan Zhang, Neutron diffraction residual strain measurements of molybdenum carbide based solid oxide fuel cell anode layers with metal oxides on Hastelloy X, Experimental Mechanics, 58(4), 2018, 585-603.

[6] R. Ahmed, H. Yu, V. Stoica, L. Edwards, J. R. Santisteban, Neutron diffraction residual strain measurements in post-treated thermal spray cermet coatings, Materials Science and Engineering: A, 498, 2008, 191-202.

[7] P. J. Withers, H. K. D. H. Bhadeshia, Residual stress. Part 1 – Measurement techniques, Materials Science and Technology, 17(4), 2001, 355-365.

Electronic copy available at: https://ssrn.com/abstract=3711244

[8] P. J. Withers, H. K. D. H. Bhadeshia, Residual stress. Part 2 – Nature and origins, Materials Science and Technology, 17(4), 2001, 366-375.

[9] R. Ahmed, M. Hadfield, S. Tobe, Residual stress analysis in thermal spray coated rolling elements, National Thermal Spray Conference, USA, ISBN 0-87170-583-4, 1996, 875-883.

[10] M. Hadfield, R. Ahmed, S. Tobe, Residual stress measurements of silicon nitride and coated tungsten carbide rolling contact elements, Surface Treatment-III, 17, 1997, 319-328.

[11] R. Ahmed, M. Hadfield, Experimental measurement of the residual stress field within thermally sprayed rolling elements, Wear, 209, 1997, 84-95.

[12] R. Ahmed, M. Hadfield, S. Tobe, Variation in residual stress fields during fatigue failure of thermal spray coatings, International Thermal Spray Conference, Canada, ISBN 0-87170-680-6, 2000, 399-406.

[13] A. M. Paradowska, A. Tremsin, J. F. Kelleher, S. Y. Zhang, S. Paddea, G. Burca, J. A. James, R. Ahmed, N. H. Faisal, F. Grazzi, G. Festa, C. Andreani, F. Civita, P. J.Bouchard, W. Kockelman, M. E. Fitzpatrick, Modern and historical engineering concerns investigated by neutron diffraction, Journal of Solid Mechanics and Materials Engineering, 6(6), 2012, 408-418.

[14] V. Stoica, R. Ahmed, M. Golshan, S. Tobe, Sliding Wear Evaluation of Hot Isostatically Pressed (HIPed) Thermal Spray Cermet Coatings, Journal of Thermal Spray Technology, 13(1), 2004, 93-107.

[15] A. Fardan, R. Ahmed, Modeling the evolution of residual stresses in thermally sprayed YSZ coating on stainless steel substrate, Journal of Thermal Spray Technology, 28(4), 2019, 717-736.

[16] M. E. Fitzpatrick, A. Lodini, Analysis of Residual Stress by Diffraction using Neutron and Synchrotron Radiation. London: Taylor and Francis, 2003.

[17] J. R. Santisteban, M. R. Daymond, J. A. James, L. Edwards, ENGIN-X: a third-generation neutron strain scanner, J. Appl. Cryst. 39, 2006, 812-825.

[18] Development and applications of residual stress measurements using neutron beams. — Vienna: International Atomic Energy Agency, 2014; http://www-pub.iaea.org/MTCD/Publications/PDF/trs477_web.pdf

[19] G. S. Schajer, Practical Residual Stress Measurement Methods, John Wiley & Sons, Ltd (2013), Online ISBN:9781118402832 (p. 1-27, p. 195-223).

[20] J. A. James, L. Edwards, Application of robot kinematics methods to the simulation and control of neutron beam line positioning systems. Nuclear Instruments and Methods in Physics Research A., 571, 2007, 709–718.

Electronic copy available at: https://ssrn.com/abstract=3711244

[21] M. T. Hutchings, P. J Withers, T. M. Holden, T. Lorentzen, Introduction to the Characterization of Residual Stress by Neutron Diffraction. Boca Raton: CRC Press, Taylor and Francis (2005).

[22] N. H. Faisal, A. Prathuru, R. Ahmed, S. Y. Zhang (2015): Neutron Diffraction Residual Strain Measurements of Plasma Sprayed Solid Oxide Fuel Cells, STFC ISIS Neutron and Muon Source, https://doi.org/10.5286/ISIS.E.58451518 (RB1510238)

[23] International Centre for Diffraction Data (ICDD) software Powder Diffraction File™ (PDF); https://www.icdd.com/pdfsearch/

[24] M. Gell, J. Wang, R. Kumar, J. Roth, C. Jiang. E. H. Jordan Higher Temperature Thermal Barrier Coatings with the Combined Use of Yttrium Aluminum Garnet and the Solution Precursor Plasma Spray Process, Journal of Thermal Spray Technology, 27, 2018, 543–555.

[25] INTERNATIONAL ORGANIZATION FOR STANDARDIZATION, Non-Destructive Testing — Standard Test Method for Determining Residual Stresses by Neutron Diffraction, ISO/TS 21432:2005, ISO, Geneva (2005).

[26] S. Y. Zhang, E. Godfrey, B. Abbey, P. Xu, Y. Tomota, D. Liljedahl, O. Zanellato, M. Fitzpatrick, J. Kelleher, S. Siano, J. Santisteban, A M. Korsunsky, Materials Structure and Strain Analysis Using Time-of-flight Neutron Diffraction, Proceedings of the World Congress on Engineering 2009 Vol II WCE 2009, July 1 - 3, 2009, London, UK, http://www.iaeng.org/publication/WCE2009/WCE2009_pp1412-1419.pdf

[27] Engin-X positioner, https://www.isis.stfc.ac.uk/Pages/ENGINX-Positioner.aspx

[28] R. B. Von Dreele, J. D. Jorgensen, C. G. Windsor, Rietveld refinement with spallation neutron powder diffraction data, Journal of Applied Crystallography, 15, 1982, 581–589.

[29] H. M. Rietveld, A profile refinement method for nuclear and magnetic structures. Journal of Applied Crystallography, 2, 1969, 65-71.

[30] N. H. Faisal, L. Mann, C. Duncan, E. Dunbar, M. Clayton, M. Frost, J. McConnachie, A. Fardan, R. Ahmed, Diametral compression test method to analyse relative surface stresses in thermally sprayed coated and uncoated circular disc specimens, Surface and Coatings Technology, 357, 2019, 497-514.

[31] W. B. Choi, L. Li, V. Luzin, R. Neiser, T. Gnaupel-Herold, H. J. Prask, S. Sampath, A. Gouldstone, Integrated characterization of cold sprayed aluminum coatings, Acta Materialia, 55, 2007, 857–866.

[32] V. Luzin, P. Spiridonov, K. Spencer, T. Gnaupel-Herold, Neutron diffraction study of macrostress and microstress in Al-Al_2O_3-based corrosion protection coating

Electronic copy available at: https://ssrn.com/abstract=3711244

obtained by cold spray (dynamic metallization), Journal of Thermal Spray Technology, 29, 2020, 1437–1454.

[33] A. M. Venter, V. Luzin, D. Marais, N. Sacks, E. N. Ogunmuyiwa, P. H. Shipway, Interdependence of slurry erosion wear performance and residual stress in WC-12wt%Co and WC-10wt%VC-12wt%Co HVOF coatings, International Journal of Refractory Metals & Hard Materials 87 (2020) 105101

[34] A. M. Venter, P. R. van Heerden, D. Marais, J. C. Raaths, MPISI: The neutron strain scanner materials probe for internal strain investigations at the SAFARI-1 research reactor, Physica B: Condensed Matter, 551, 2018, 417–421

[35] O. Kirstein, V. Luzin, U. Garbe, The strain-scanning diffractometer Kowari, Neutron News, 20(4), 2009 34-36.

[36] V. Luzin, A. Vackel, A. Valarezo, S. Sampath, Neutron through-thickness stress measurements in coatings with high spatial resolution, Materials Science Forum, 905, 2017, 165-173.

[37] O. P. Oladijo, V. Luzin, T. P. Ntsoane, Thermally sprayed Inconel 625 coating on 304 stainless steel: a neutron diffraction stress analysis, Procedia Manufacturing, 35, 2019, 1234-1239.

[38] O. P. Oladijo, V. Luzin, N. B. Maledi, K. Setswalo, T. P. Ntsoane, H. Abe, Residual stress and wear resistance of HVOF Inconel 625 coating on SS304 steel substrate, Journal of Thermal Spray Technology, 29, 2020, 1382–1395.

[39] G. M. Smith, J. Saputo, V. Luzin, S. Sampath, Observation of residual stress and fatigue behavior of structurally integrated thermally sprayed nickel coatings, Journal of Thermal Spray Technology, 29, 2020, 1229–1241.

[40] M. Saleh, V. Luzin, K. Spencer, Analysis of the residual stress and bonding mechanism in the cold spray technique using experimental and numerical methods, Surface & Coatings Technology, 252, 2014, 15–28.

[41] V. Luzin, O. Kirstein, S. H. Zahiri, D. Fraser, Residual stress buildup in Ti components produced by cold spray additive manufacturing (CSAM), Journal of Thermal Spray Technology, 29, 2020, 1498–1507.

[42] S. Y. Kim, V. Luzin, M. L. Sesso, J. Thornton, S. Gulizia, The effect of low temperature range heat treatment on the residual stress of cold gas dynamic sprayed Inconel 718 coatings via neutron diffraction, Journal of Thermal Spray Technology, 29, 2020, 1477–1497.

[43] J. Gibmeier, H. C. Back, M. Mutter, F. Vollert, J. Rebelo-Kornmeier, R. Mücke, R. Vaßen, Study of stability of microstructure and residual strain after thermal loading of plasma sprayed YSZ by through surface neutron scanning, Physica B: Condensed Matter, 551, 2018, 69–78

Electronic copy available at: https://ssrn.com/abstract=3711244

[44] C. Lyphout, P. Nylen, A. Manescu, and T. Pirling, Residual stresses distribution through thick HVOF sprayed inconel 718 coatings, Journal of Thermal Spray Technology, 17(5-6), 2008, 915-923.

[45] O. Kovářík, P. Haušild, J. Siegl, Z. Pala, J. Matějíček, V. Davydov, The influence of plasma sprayed multilayers of Cr2O3and Ni10wt%Al on fatigue resistance, Surface and Coatings Technology, 251, 2014, 143-150.

[46] V. Luzin, H.-J. Prask, T. Gnaupel-Herold, S. Sampath, Use of neutron diffraction for stress measurements in thin and thick thermal sprayed coatings, International Heat Treatment and Surface Engineering, 4(1), 2010, 17-24.

[47] L. Li, A. Vaidya, T. Streibl, S. Sampath, A. Gouldstone, V. Luzin, H. J. Prask, Residual stress analysis of thermal sprayed molybdenum deposit, Materials Science Forum, 490-491, 2005, 607-612.

[48] V. Luzin, K. Spencer, M.-X. Zhang, Residual stress and thermo-mechanical properties of cold spray metal coatings, Acta Materialia, 59 (2011) 1259–1270.

[49] M. Ceretti, M. Michaud, M. Perrin, A. Lodini, Residual stress measurement in a plasma semi-transferred arc coating by neutron and x-ray diffraction, Experimental Technique, 19(3), 1995, 17-21.

[50] C. A. Dragolici (April 6th, 2016). Experimental Methods in the Study of Neutron Scattering at Small Angles, Neutron Scattering, Waldemar Alfredo Monteiro, IntechOpen, DOI: 10.5772/62184

[51] T. Keller, W. Wagner, J. Ilavsky, N. Margadant, S. Siegmann, G. Barbezat, J. Pisacka, and R. Enzl, Characterization of void morphologies in thermally sprayed metallic deposits using scattering techniques, in: PSI Scientific and Technical Report 2001, *Vol.* VI, *ISBN/ISSN*. 1423-7350, p. 91-923

[52] D. Sen, A. K. Patra, S. Mazumder, S. Ramanathan, Pore growth during initial and intermediate stages of sintering in ZrO_2–3 mol% Y_2O_3 compact: A small-angle neutron scattering investigation. J. Alloys Compounds, 361, 2003, 270–275.

[53] S. Takajo, K. J. Hollis, D. R. Cummins, E. L. Tegtmeier, D. E. Dombrowski, S. C. Vogel, Texture evolution in U-10Mo nuclear fuel foils during plasma spray coating with Zr, Quantum Beam Science, 2, 2018,12.

[54] H. G. Brokmeier, Neutron diffraction texture analysis, Physica B: Condensed Matter, 234-236, 1997, 977-979.

[55] S. Jakani, Marie-Hélène Mathon, A. Benmarouane, A. Lodini, Neutron diffraction study of nano-hydroxyapatite coatings on titanium substrates, Journal of Neutron Research, 15(3), 2007, 225-229.

[56] T. Liu, M. D. Vaudin, J. R. Bunn, T. Ungar, L. N. Brewe, Quantifying dislocation density in Al-Cu coatings produced by coldspray deposition, Acta Materialia, 193, 2020, 115-124.

Electronic copy available at: https://ssrn.com/abstract=3711244

[57] T. Hussain, T. L. Lee, D. J. Martin, K. Derelizade, N. H. Faisal, T. Owoseni, J. Kelleher, J. Murray, M. Bai; (2017): Residual strain measurement in suspension based thermal sprayed nanostructured alumina coatings, STFC ISIS Neutron and Muon Source, https://doi.org/10.5286/ISIS.E.86391325

[58] T. Hussain, J. Murray, T. L. Lee, T. Owoseni, M. Bai, N. H. Faisal, D. J. Martin, K. Derelizade, J. Kelleher; (2018): Residual strain measurement in suspension based thermal sprayed nanostructured alumina coatings, STFC ISIS Neutron and Muon Source, https://doi.org/10.5286/ISIS.E.90880498

[59] T. Hussain, D. J. Martin, T. L. Lee, K. Derelizade, J. Kelleher, T. Owoseni, N. H. Faisal, J. Pulsford; (2018): Neutron Diffraction Strain Analysis of Ceramic Coatings from Suspension Thermal Spray, STFC ISIS Neutron and Muon Source, https://doi.org/10.5286/ISIS.E.98023160

[60] A. A. Abubakar, A. F. M. Arif, K. S. Al-Athel, S. S. Akhtar, J. Mostaghimi, Modeling Residual Stress Development in Thermal Spray Coatings: Current Status and Way Forward, Journal of Thermal Spray Technology, 26, 2017, 1115-1145.

[61] J. Mathew, J. Griffin, M. Alamaniotis, S. Kanarachos, M.E. Fitzpatrick, Prediction of welding residual stresses using machine learning: Comparison between neural networks and neuro-fuzzy systems, Applied Soft Computing, 70, 2018, 131-146.

[62] F. Uzun, C. Papadaki, Z. Wang, A. M. Korsunsky, Neutron strain scanning for experimental validation of the artificial intelligence based eigenstrain contour method, Mechanics of Materials, 143, 2020, 103316.

Electronic copy available at: https://ssrn.com/abstract=3711244

Table Caption

Table 1. Neutron diffractometers for strain measurement and microstructure (with thermal spray coating examples only).

Figure Captions

Fig. 1. (a) Air plasma spraying in coating chamber (Monitor Coatings Ltd, Tyne & Wear, UK, 2005), (b) scheme of layer deposition during single and multi-pass thermal spraying, and (c) factor of net residual stress formation in thermal spray coating (adapted from [6]).

Fig. 2. Engin-X neutron strain testing facility (ISIS Neutron Source, Science and Technology Facilities Council, Rutherford Appleton Laboratory, Didcot, UK (dated: 2 April 2015).

Fig. 3. Bragg scattering geometry (adapted from [18]).

Fig. 4. Typical TOF neutron diffraction pattern near the coating-substrate interface in the air plasma spray coating part (including *hkl* peaks): (a) Mo-Mo_2C/Al_2O_3 coating (b) individual peak least-squares refinement of a Mo peak & showing d-spacing shift scheme, and (c) Hastelloy®X substrate of corresponding Mo-Mo_2C/Al_2O_3 coating (used as $d_{hkl}^0$for Hastelloy®X substrate). The elastic strain is calculated from the shift in the peak positions defined through a least-squares refinement (in (b)) [5, 22].

Fig. 5. Scheme of strain measurement on disc shaped coated sample at Engin-X.

Fig. 6. Gauge volume as seen vertically: Through thickness neutron diffraction residual strain measurement: (a) recommended scheme, and (b) cross-section image of 250 μm thick Mo-Mo_2C/Al_2O_3 coating on 4.7 mm thick Hastelloy®X substrate (showing features near the surfaces and interface and practical measurement positions from top of the coating surface).

Fig. 7. Measuring residual strain using neutron diffraction at Engin-X.

Fig. 8. Fast scanning: Sample vertical scan (z-scan) at the start of the air plasma sprayed Mo-Mo_2C/Al_2O_3 coating surface (with Hastelloy®X substrate) (refer Appendix-Supplementary Data-RB1510238 [22].

Fig. 9. (a) Measuring residual strain using neutron diffraction, (b) crushed powder, and (b) crushed powder filled Vanadium tube for d_0 measurement [5].

Fig. 10. Residual strain analysis based on single peak fitting routine analysis for neutron diffraction residual strain in Mo-Mo_2C/Al_2O_3 (250 μm thick coatings on 4.7 mm thick Hastelloy®X substrate): (a) for individual peaks, and (b) average of all individual peaks [5].

Fig. 11. Residual stress analysis: (a) scheme of nanoindentation array (coating-substrate cross-section surface) to measure elastic modulus for residual stress analysis,

Electronic copy available at: https://ssrn.com/abstract=3711244

and (b) residual stress analysis based on average of all individual peaks in Mo-Mo_2C/Al_2O_3 (250 μm thick coatings on 4.7 mm thick Hastelloy®X substrate) [5].

Fig. 12. Normalised stress analysis based on average of all individual peaks in Mo-Mo_2C/Al_2O_3 (250 μm thick coatings on 4.7 mm thick Hastelloy®X substrate) [note: yield stress of the Hastelloy-X® substrate is taken as 385 MPa and for Mo-Mo_2C/Al_2O_3 it is taken as 770 MPa (at zero plastic strain)].

Electronic copy available at: https://ssrn.com/abstract=3711244

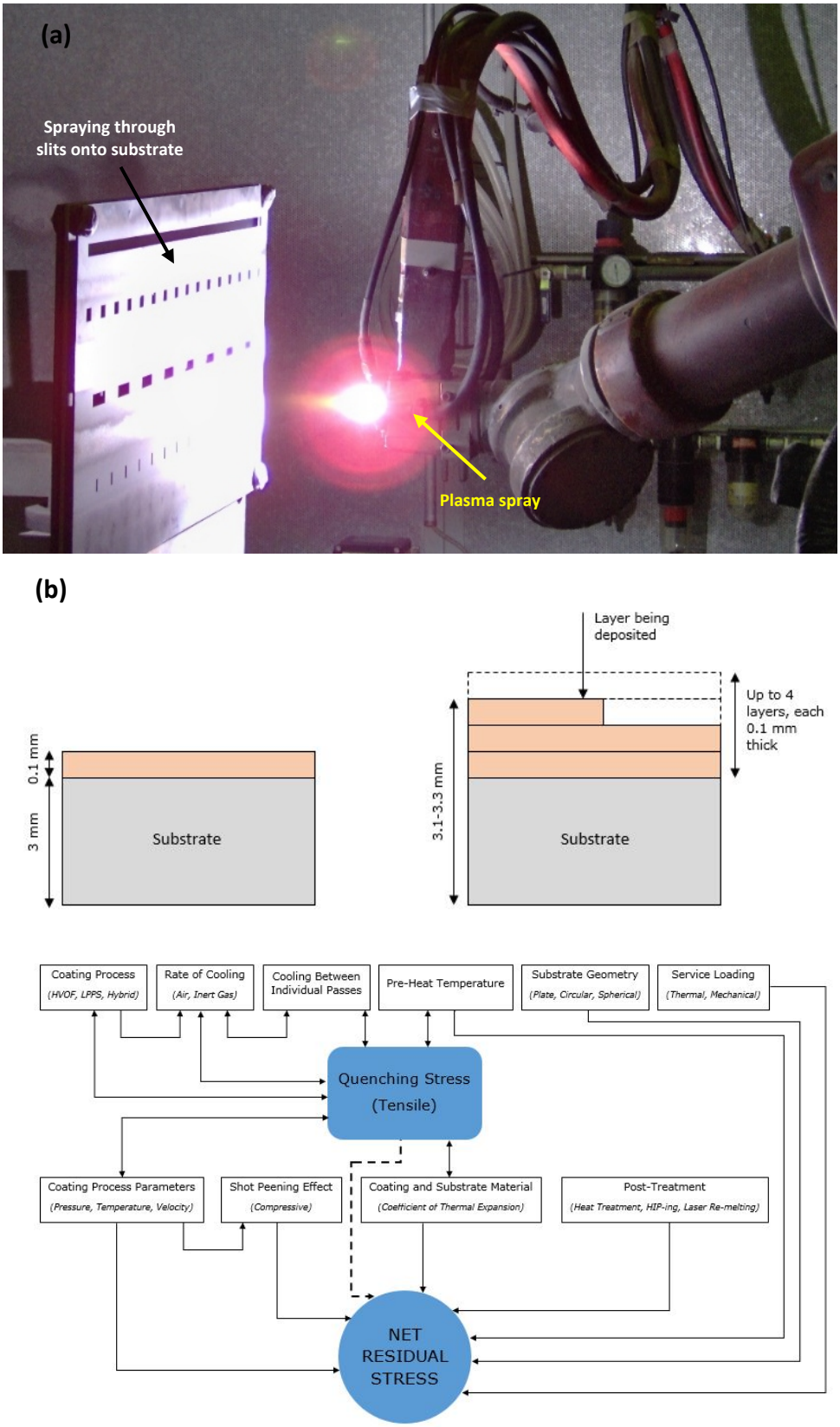

Fig. 1. (a) Air plasma spraying in coating chamber (Monitor Coatings Ltd, Tyne & Wear, UK, 2005), (b) scheme of layer deposition during single and multi-pass thermal spraying, and (c) factor of net residual stress formation in thermal spray coating (adapted from [6]).

Electronic copy available at: https://ssrn.com/abstract=3711244

Fig. 2. Engin-X neutron strain testing facility (ISIS Neutron Source, Science and Technology Facilities Council, Rutherford Appleton Laboratory, Didcot, UK (dated: 2 April 2015).

Electronic copy available at: https://ssrn.com/abstract=3711244

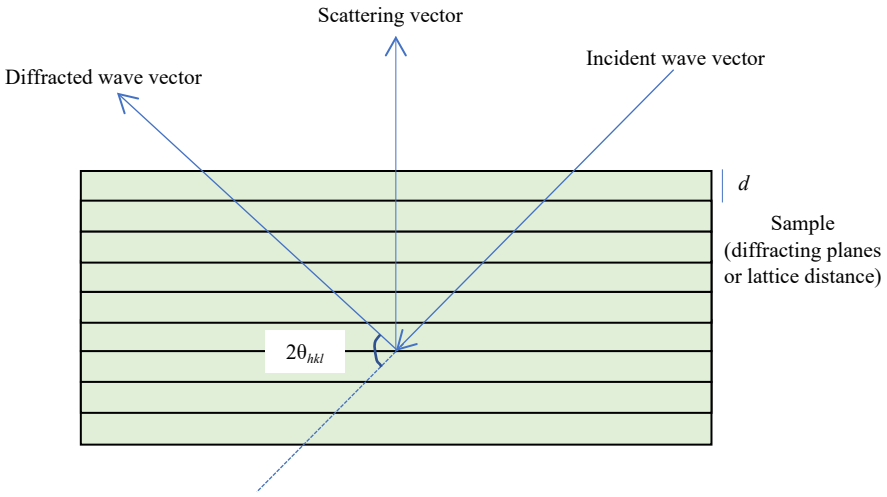

Fig. 3. Bragg scattering geometry (adapted from [18]).

Electronic copy available at: https://ssrn.com/abstract=3711244

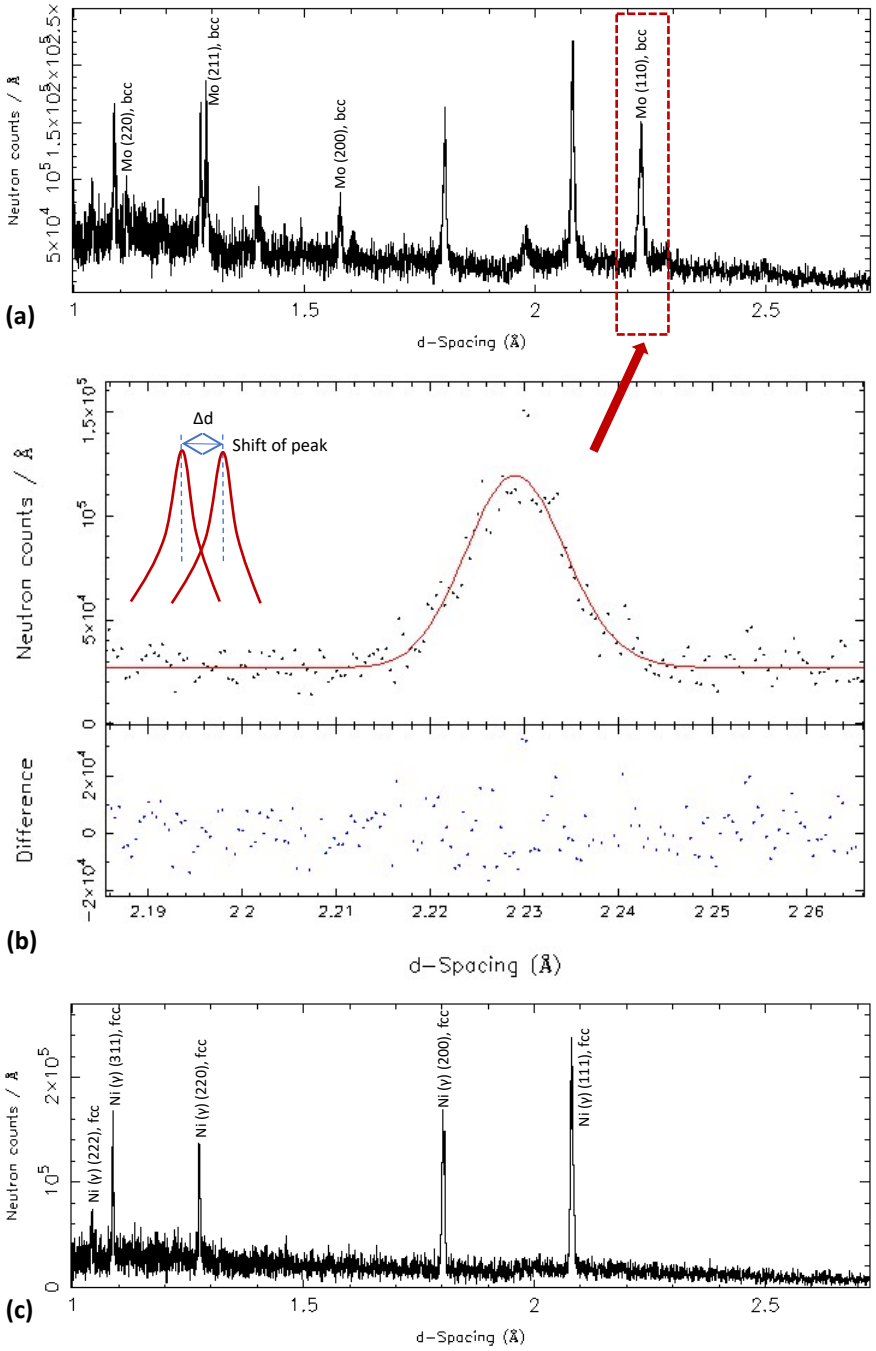

Fig. 4. Typical TOF neutron diffraction pattern near the coating-substrate interface in the air plasma spray coating part (including *hkl* peaks): (a) Mo-Mo_2C/Al_2O_3 coating (b) individual peak least-squares refinement of a Mo peak & showing d-spacing shift scheme, and (c) Hastelloy®X substrate of corresponding Mo-Mo_2C/Al_2O_3 coating (used as $d_{hkl}^0$for Hastelloy®X substrate). The elastic strain is calculated from the shift in the peak positions defined through a least-squares refinement (in (b)) [5, 22].

Electronic copy available at: https://ssrn.com/abstract=3711244

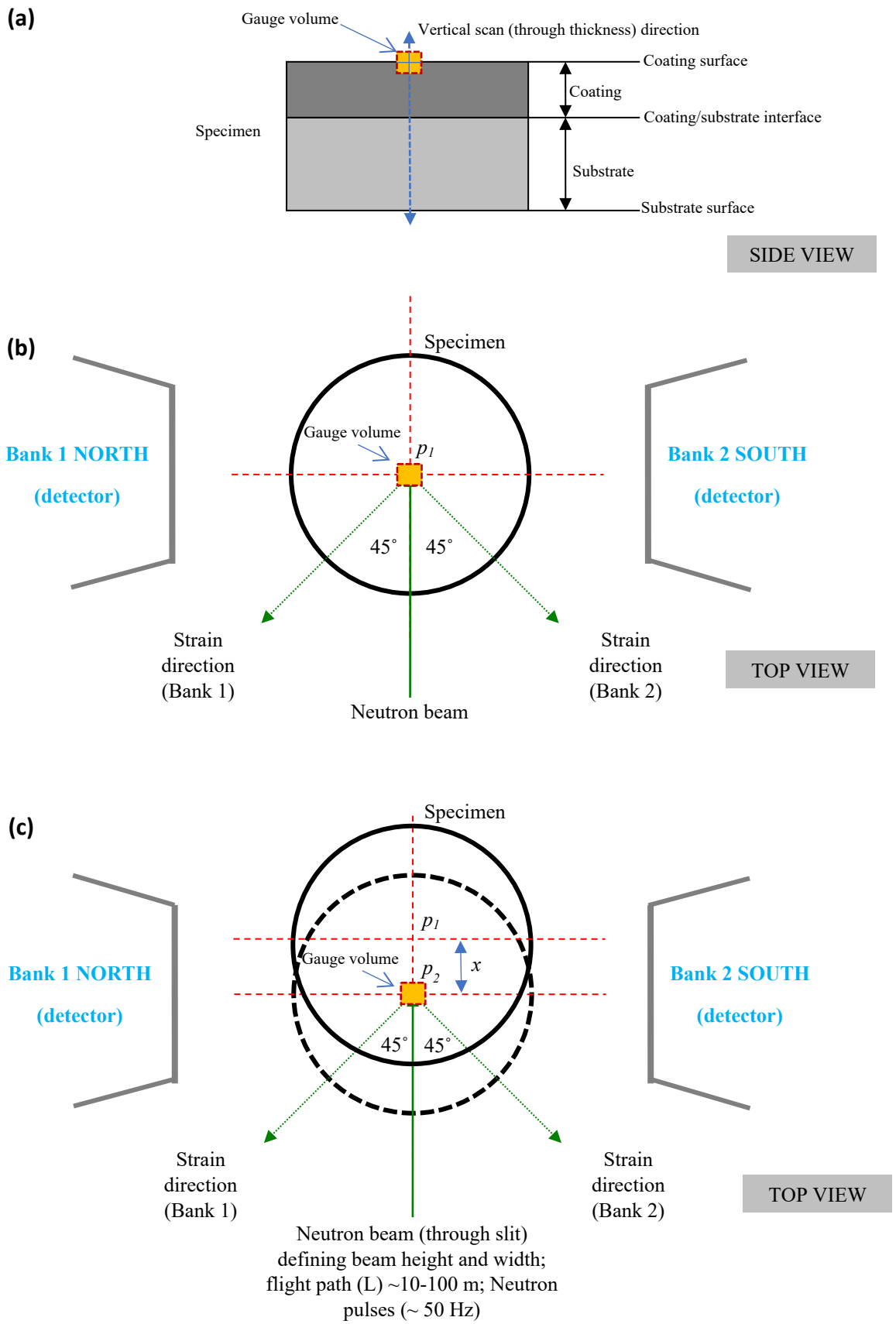

Fig. 5. Scheme of strain measurement on disc shaped coated sample at Engin-X.

Electronic copy available at: https://ssrn.com/abstract=3711244

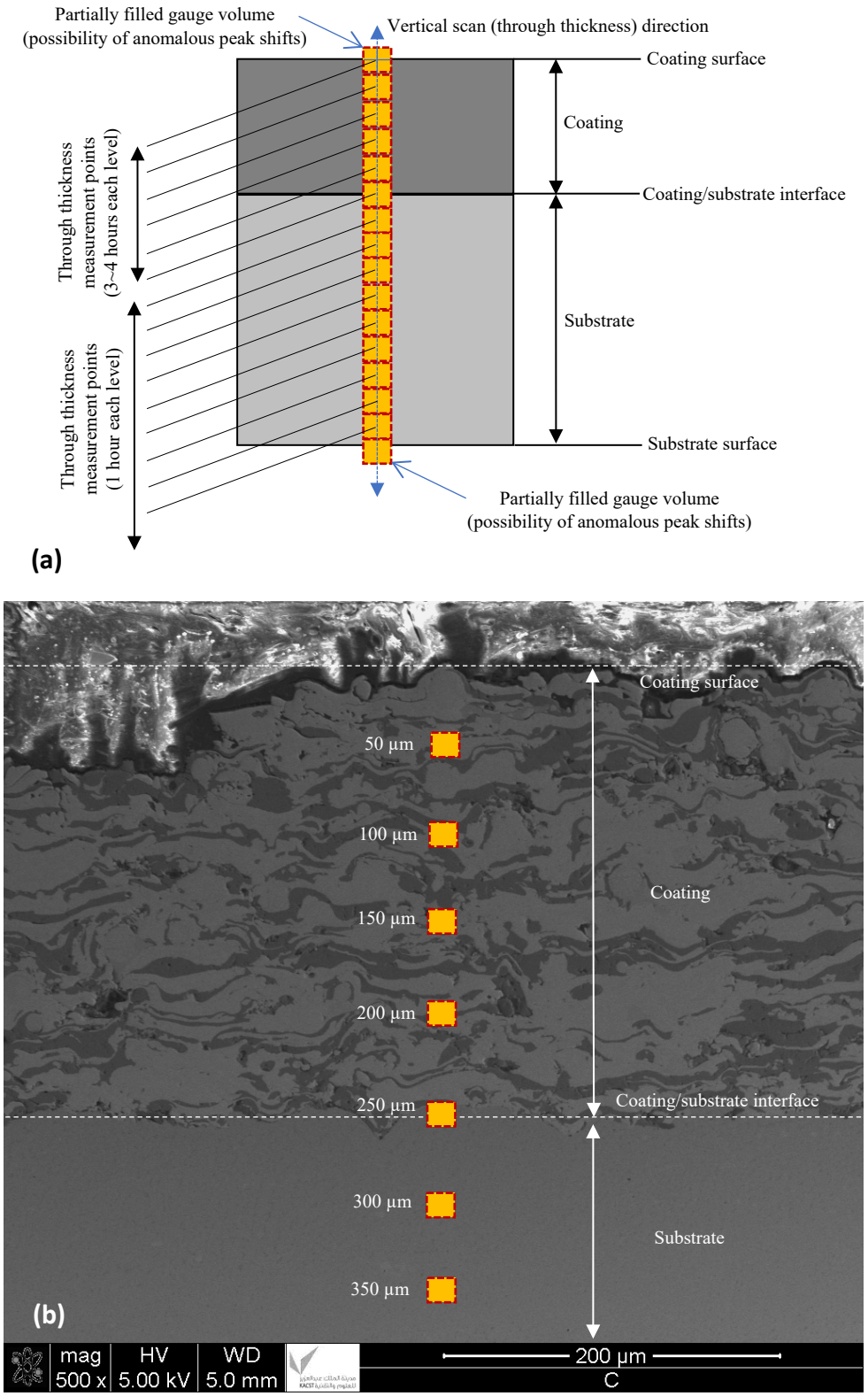

Fig. 6. Gauge volume as seen vertically: Through thickness neutron diffraction residual strain measurement: (a) recommended scheme, and (b) cross-section image of 250 µm thick Mo-Mo_2C/Al_2O_3 coating on 4.7 mm thick Hastelloy®X substrate (showing features near the surfaces and interface and practical measurement positions from top of the coating surface).

Electronic copy available at: https://ssrn.com/abstract=3711244

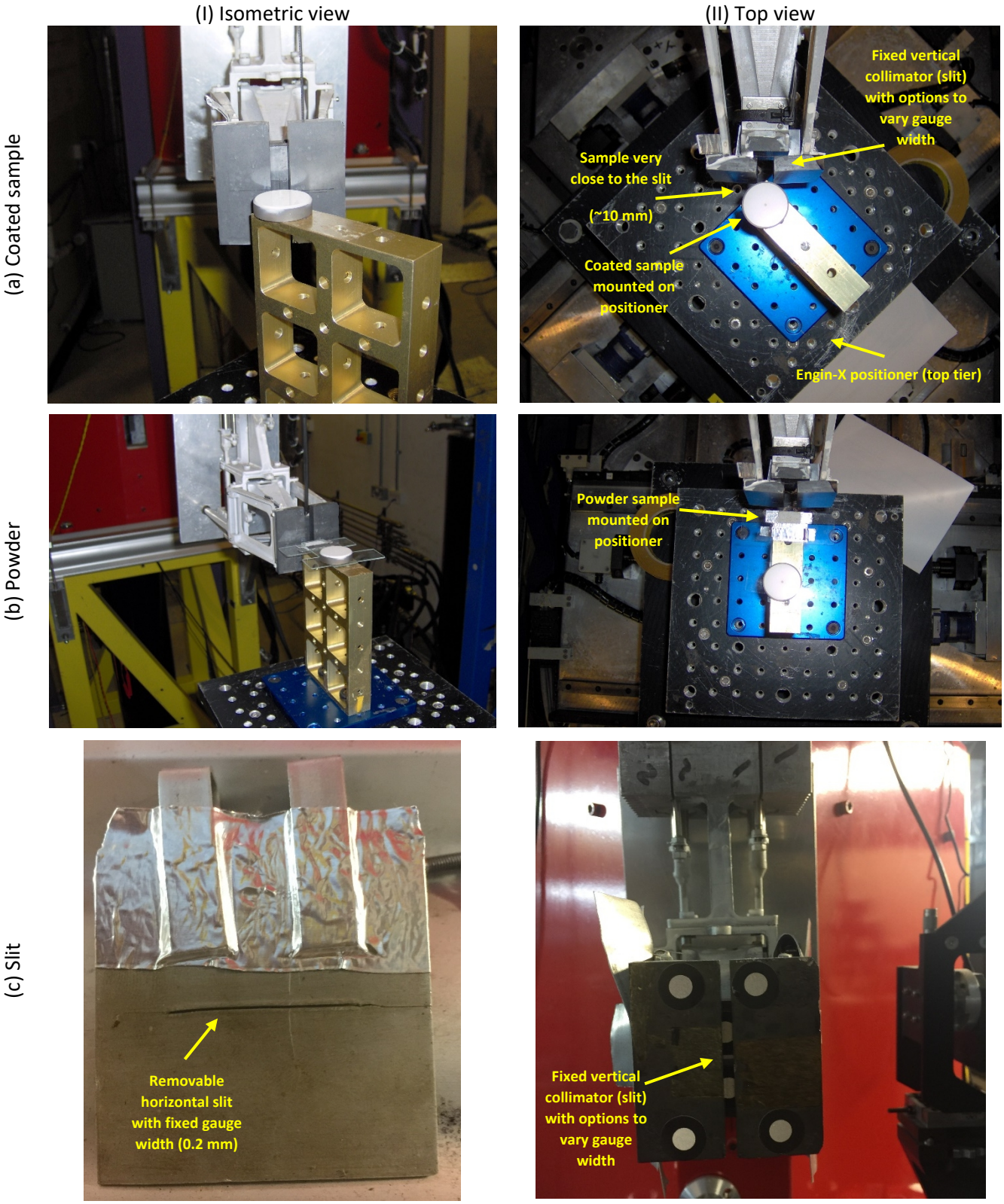

Fig. 7. Measuring residual strain using neutron diffraction at Engin-X.

Electronic copy available at: https://ssrn.com/abstract=3711244

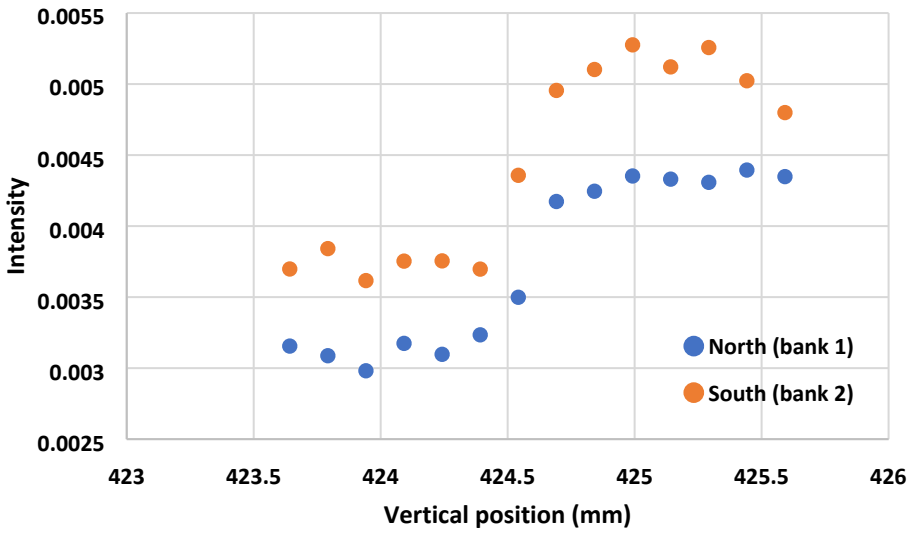

Fig. 8. Fast scanning: Sample vertical scan (z-scan) at the start of the air plasma sprayed Mo-Mo_2C/Al_2O_3 coating surface (with Hastelloy®X substrate) (refer Appendix-Supplementary Data-RB1510238 [22].

Electronic copy available at: https://ssrn.com/abstract=3711244

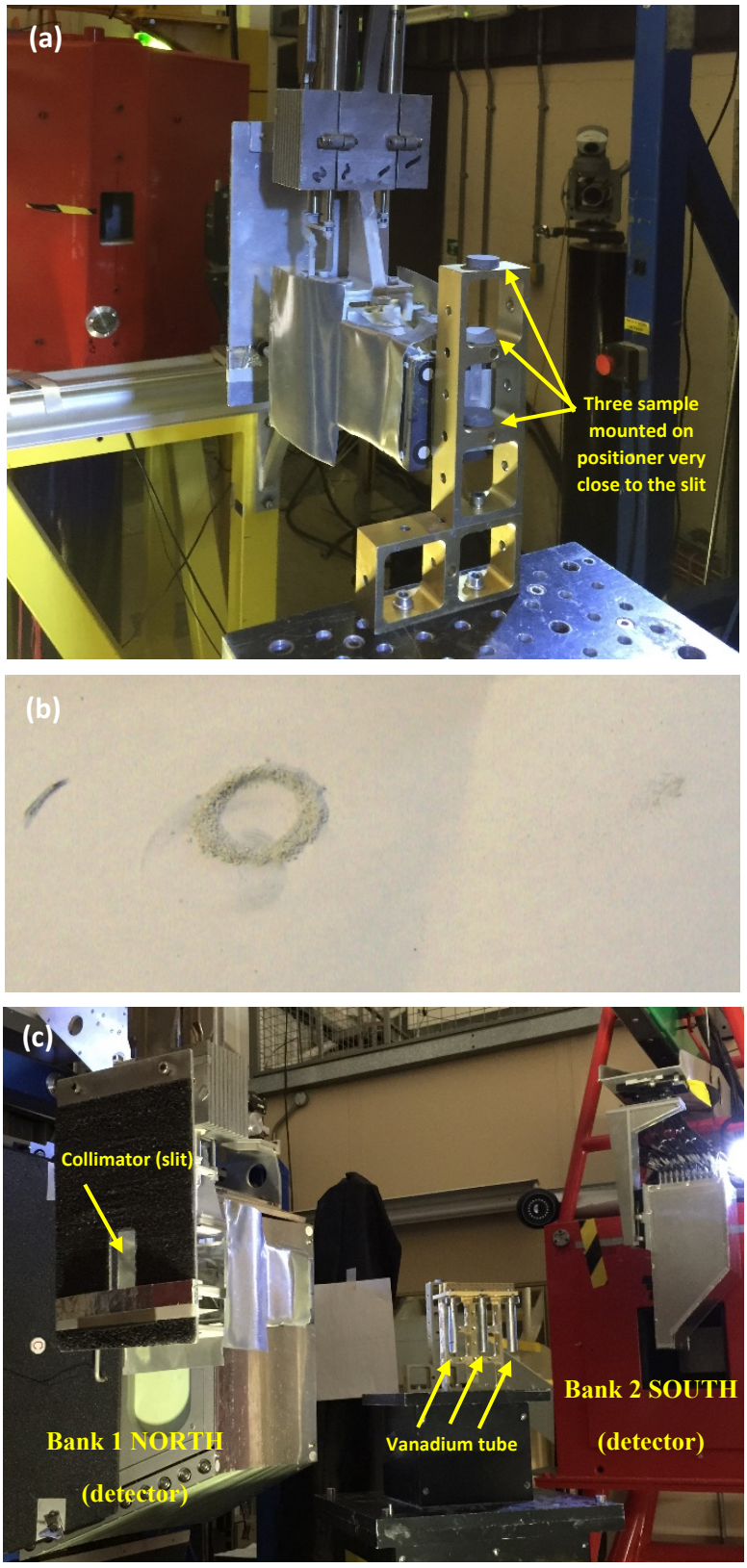

Fig. 9. (a) Measuring residual strain using neutron diffraction, (b) crushed powder, and (b) crushed powder filled Vanadium tube for d_0 measurement [5].

Electronic copy available at: https://ssrn.com/abstract=3711244

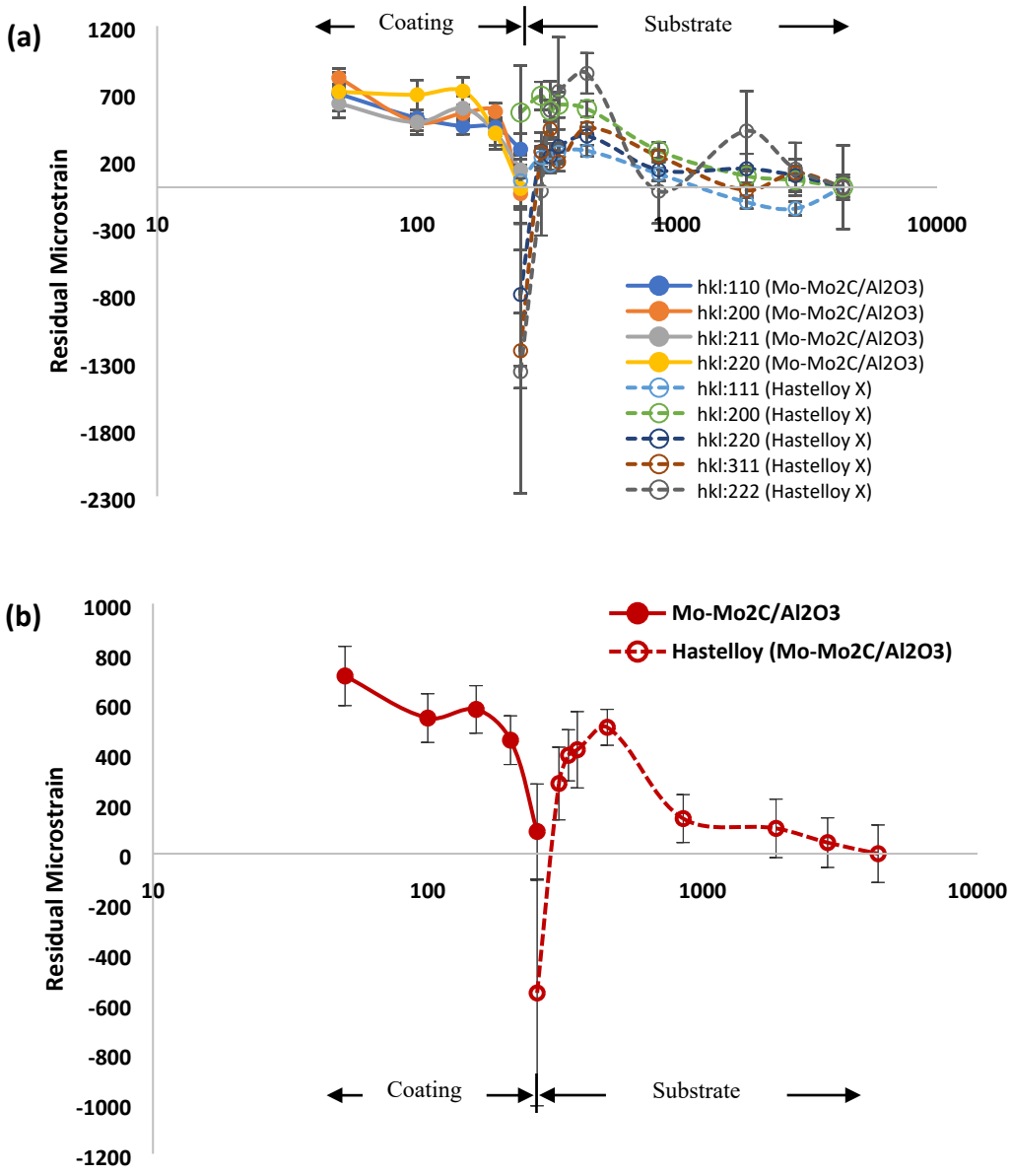

Fig. 10. Residual strain analysis based on single peak fitting routine analysis for neutron diffraction residual strain in Mo-Mo_2C/Al_2O_3 (250 μm thick coatings on 4.7 mm thick Hastelloy®X substrate): (a) for individual peaks, and (b) average of all individual peaks [5].

Electronic copy available at: https://ssrn.com/abstract=3711244

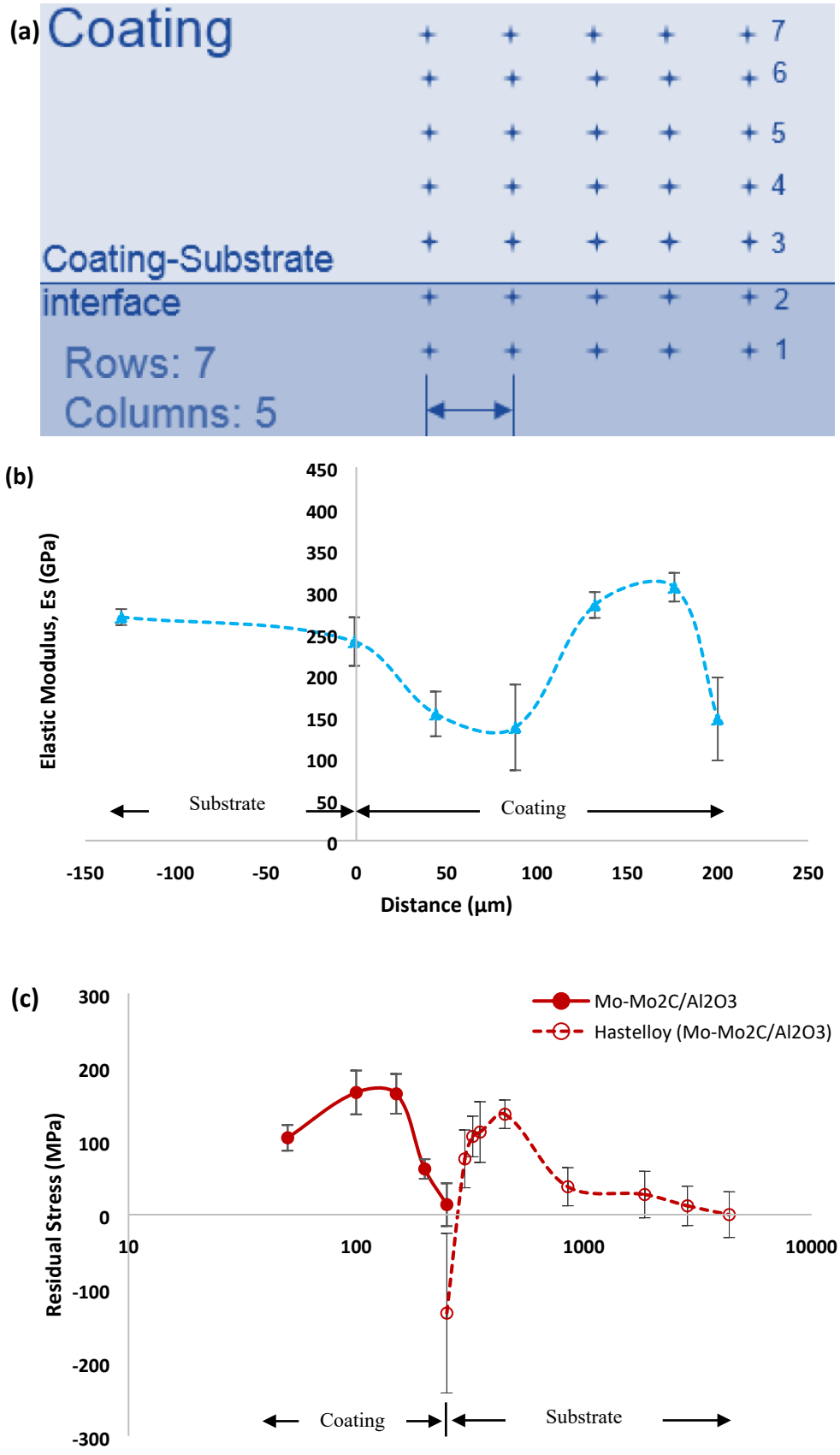

Fig. 11. Residual stress analysis: (a) scheme of nanoindentation array (coating-substrate cross-section surface) to measure elastic modulus for residual stress analysis, and (b) residual stress analysis based on average of all individual peaks in Mo-Mo_2C/Al_2O_3 (250 µm thick coatings on 4.7 mm thick Hastelloy®X substrate) [5].

Electronic copy available at: https://ssrn.com/abstract=3711244

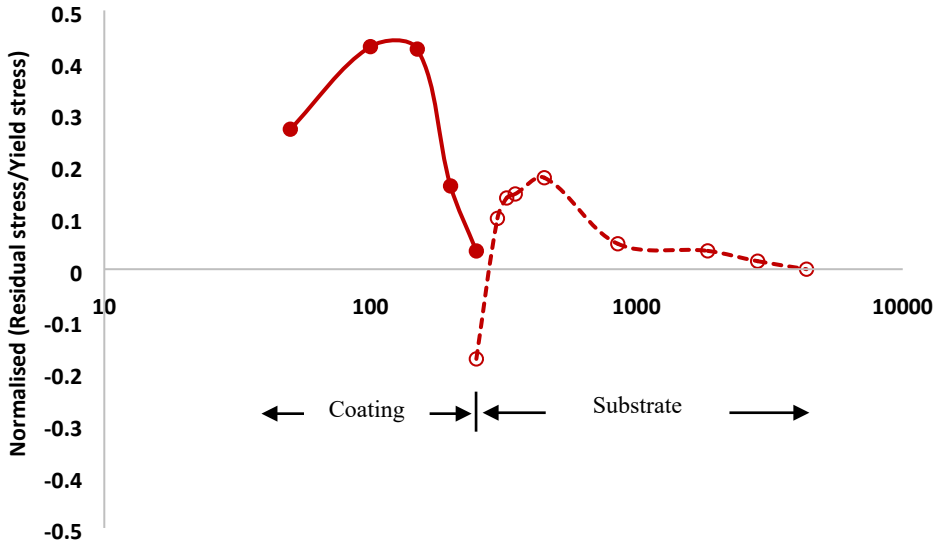

Fig. 12. Normalised stress analysis based on average of all individual peaks in Mo-Mo_2C/Al_2O_3 (250 μm thick coatings on 4.7 mm thick Hastelloy®X substrate) [note: yield stress of the Hastelloy-X® substrate is taken as 385 MPa and for Mo-Mo_2C/Al_2O_3 it is taken as 770 MPa (at zero plastic strain)].

Electronic copy available at: https://ssrn.com/abstract=3711244

Science & Technology Facilities Council
ISIS Neutron and Muon Source

Finding d-spacing from neutron spectra

[OpenGenie & HDF Explorer]

Open Genie and GSAS based analysis suite for ENGIN-X (Windows XP / 7)
Source: https://www.isis.stfc.ac.uk/Pages/EnginX-Software.aspx

Dr Nadimul Faisal

School of Engineering, Robert Gordon University, Aberdeen

n.h.faisal@rgu.ac.uk

Electronic copy available at: https://ssrn.com/abstract=3711244

Basic Engin-X OpenGenie Commands

• batch_focus;	Focus all runs
• analyze_scan;	Finds peak and analysis in group, no TOF, gives all lattice parameter
• analyze_scan/peaks;	Finds peak and analysis in group, with TOF, gives all lattice parameter
• fit_peak;	Fits the peak and difference
• fit_peak/d;	Finds d-spacing
• d w;	To plot d-spacing against intensity from the .his file
• d w;	To plot d-spacing against intensity from the .raw file

Electronic copy available at: https://ssrn.com/abstract=3711244

Engin-X routines

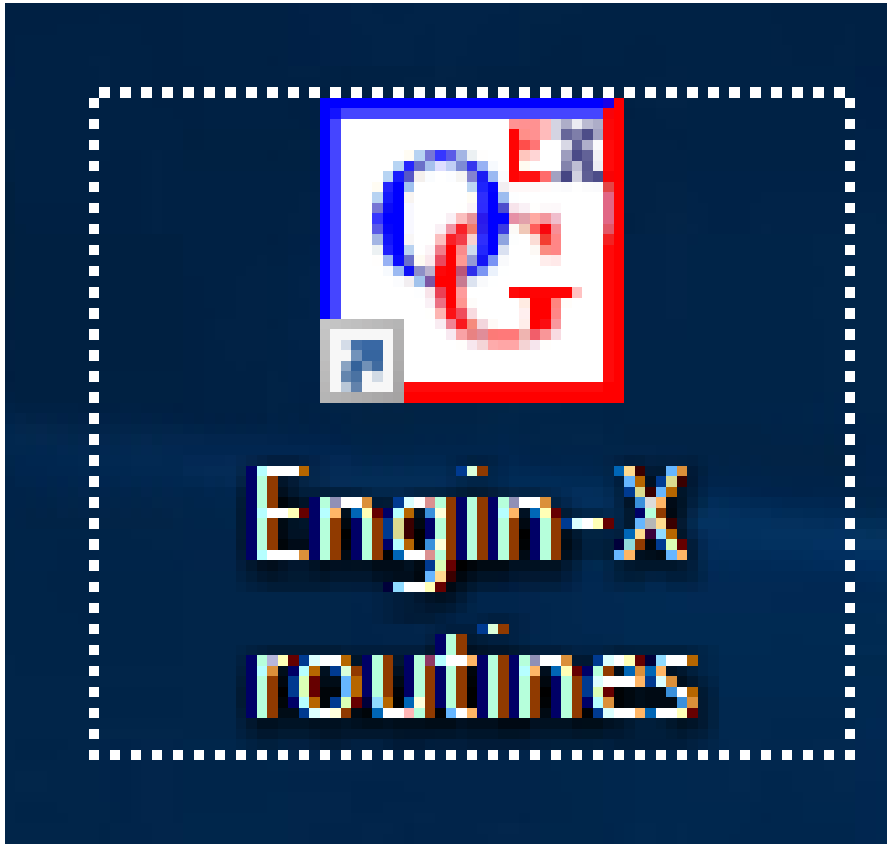

Electronic copy available at: https://ssrn.com/abstract=3711244

C:\Engin-X\focus\

Use (batch_focus) to focus all files;

Note: Copy all focused files in the focus folder;

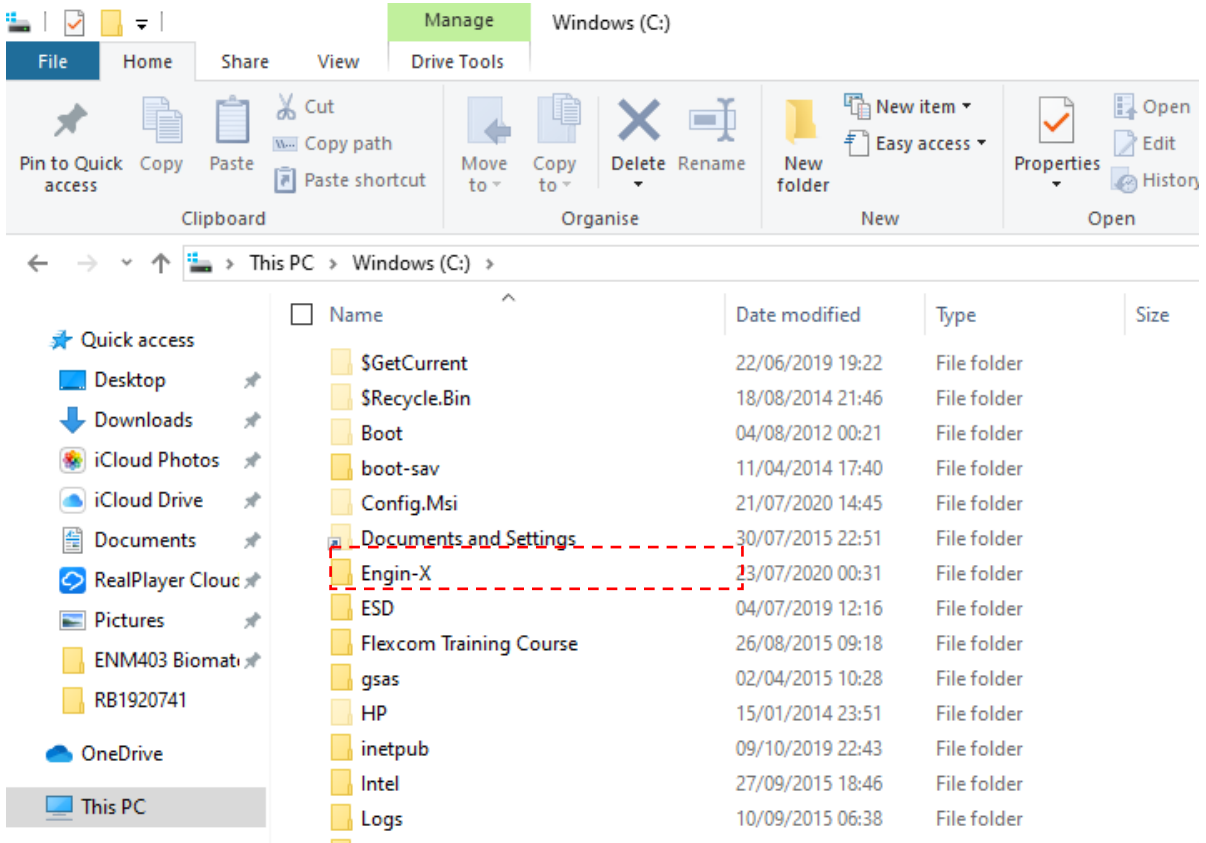

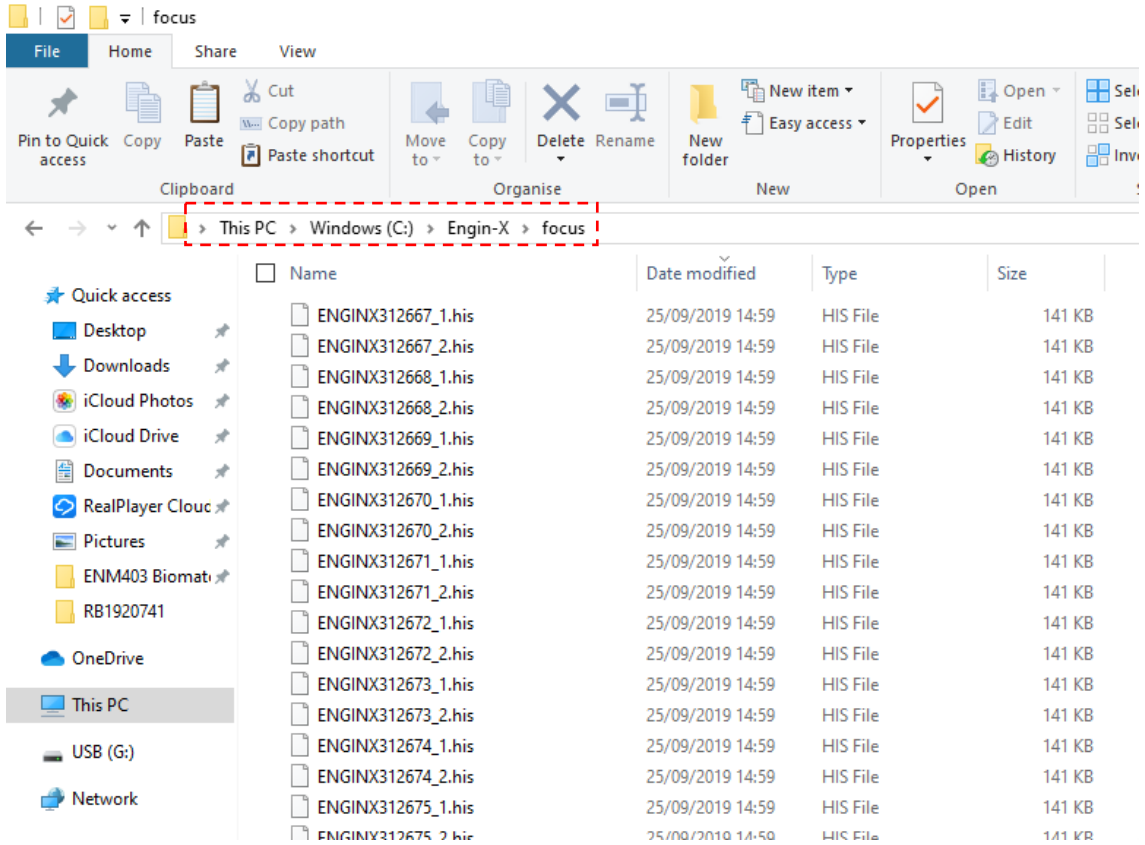

Electronic copy available at: https://ssrn.com/abstract=3711244

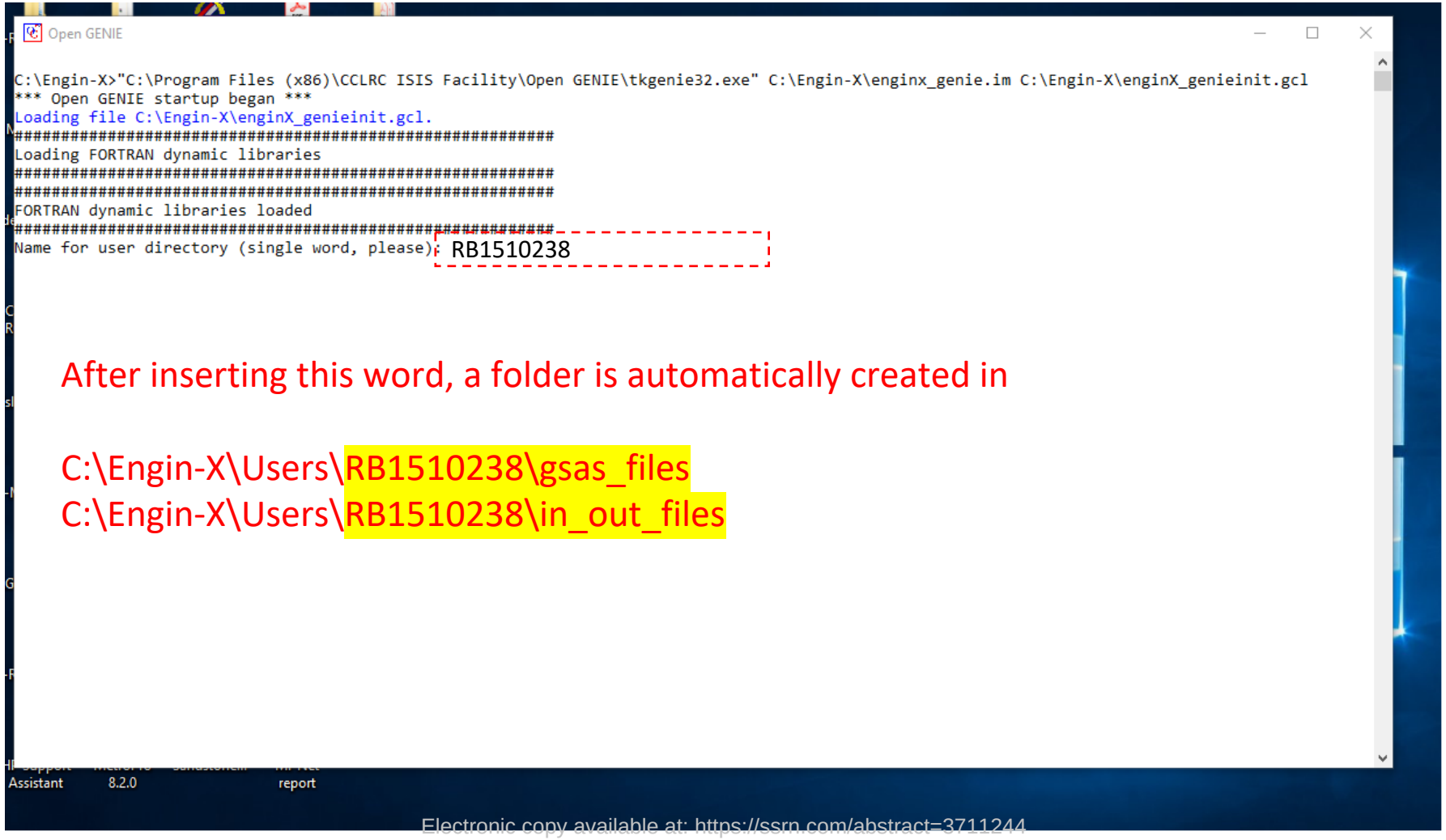

After inserting this word, a folder is automatically created in

C:\Engin-X\Users\RB1510238\gsas_files
C:\Engin-X\Users\RB1510238\in_out_files

Electronic copy available at: https://ssrn.com/abstract=3711244

Open GENIE

```
C:\Engin-X>"C:\Program Files (x86)\CCLRC ISIS Facility\Open GENIE\tkgenie32.exe" C:\Engin-X\enginx_genie.im C:\Engin-X\enginX_genieinit.gcl
*** Open GENIE startup began ***
Loading file C:\Engin-X\enginX_genieinit.gcl.
############################################################
Loading FORTRAN dynamic libraries
############################################################
############################################################
FORTRAN dynamic libraries loaded
############################################################
Name for user directory (single word, please): RB1510238
A subdirectory or file C:\Engin-X\Users\RB1510238\in_out_files\ already exists.
######## User directories ######################
GSAS files directory: C:\Engin-X\Users\RB1510238\gsas_files\
Input/Output directory: C:\Engin-X\Users\RB1510238\in_out_files\


Open GENIE successfully started at 23-Jul-2020 02:06:23+0100

######## System directories ############################
ENGINX root directory: C:\Engin-X\
Banks definition directory: C:\Engin-X\par\
Raw Data directory: C:\Engin-X\raw_data\
Focussed Data directory: C:\Engin-X\focus\
GCL code directory: C:\Engin-X\genie\gcl\

######## User directories ############################
GSAS files directory: C:\Engin-X\Users\RB1510238\gsas_files\
Input/Output directory: C:\Engin-X\Users\RB1510238\in_out_files\

Loading Smalltalk image from "C:\Engin-X\enginx_genie.im"
Loading TCL commands (if needed) from "C:\Program Files (x86)\CCLRC ISIS Facility\Open GENIE\\src\tcl\interface.tcl"

Open GENIE V2.3-BUILD-5776 (2010/02/24 15:57:01)
[Linked] Feb 24 2010 19:43:44 [library version] 1.2
(Running on x86:Windows_NT:6.2 - built with MS Visual C++ V5.0 or greater)

   ************************************************************************
   *  Copyright (C) 1996-2002 CCLRC Rutherford Appleton Lab.              *
   *  Open GENIE comes with ABSOLUTELY NO WARRANTY; for details           *
   *  type `warranty'.  This is free software, and you are welcome        *
   *  to redistribute it under certain conditions; type `licence'         *
```


Electronic copy available at: https://ssrn.com/abstract=3711244

```
Open GENIE
############################################################
Name for user directory (single word, please): RB1510238
A subdirectory or file C:\Engin-X\Users\RB1510238\in_out_files\ already exists.
######## User directories ######################
GSAS files directory: C:\Engin-X\Users\RB1510238\gsas_files\
Input/Output directory: C:\Engin-X\Users\RB1510238\in_out_files\



Open GENIE successfully started at 23-Jul-2020 01:04:09+0100


######## System directories ############################
ENGINX root directory: C:\Engin-X\
Banks definition directory: C:\Engin-X\par\
Raw Data directory: C:\Engin-X\raw_data\
Focussed Data directory: C:\Engin-X\focus\
GCL code directory: C:\Engin-X\genie\gcl\

######## User directories ############################
GSAS files directory: C:\Engin-X\Users\RB1510238\gsas_files\
Input/Output directory: C:\Engin-X\Users\RB1510238\in_out_files\

Loading Smalltalk image from "C:\Engin-X\enginx_genie.im"
Loading TCL commands (if needed) from "C:\Program Files (x86)\CCLRC ISIS Facility\Open GENIE\\src\tcl\interface.tcl"

Open GENIE V2.3-BUILD-5776 (2010/02/24 15:57:01)
[Linked] Feb 24 2010 19:43:44 [library version] 1.2
(Running on x86:Windows_NT:6.2 - built with MS Visual C++ V5.0 or greater)

   ************************************************************************
   *  Copyright (C) 1996-2002 CCLRC Rutherford Appleton Lab.              *
   *  Open GENIE comes with ABSOLUTELY NO WARRANTY; for details           *
   *  type `warranty'.  This is free software, and you are welcome        *
   *  to redistribute it under certain conditions; type `licence'         *
   *  for details.                                                        *
   ************************************************************************

>> analyze_scan
```


Electronic copy available at: https://ssrn.com/abstract=3711244

```
Open GENIE
Raw Data directory: C:\Engin-X\raw_data\
Focussed Data directory: C:\Engin-X\focus\
GCL code directory: C:\Engin-X\genie\gcl\

######## User directories ############################
GSAS files directory: C:\Engin-X\Users\RB1510238\gsas_files\
Input/Output directory: C:\Engin-X\Users\RB1510238\in_out_files\

Loading Smalltalk image from "C:\Engin-X\enginx_genie.im"
Loading TCL commands (if needed) from "C:\Program Files (x86)\CCLRC ISIS Facility\Open GENIE\\src\tcl\interface.tcl"

Open GENIE V2.3-BUILD-5776 (2010/02/24 15:57:01)
[Linked] Feb 24 2010 19:43:44 [library version] 1.2
(Running on x86:Windows_NT:6.2 - built with MS Visual C++ V5.0 or greater)

   ********************************************************************
   *  Copyright (C) 1996-2002 CCLRC Rutherford Appleton Lab.          *
   *  Open GENIE comes with ABSOLUTELY NO WARRANTY; for details       *
   *  type `warranty'.  This is free software, and you are welcome    *
   *  to redistribute it under certain conditions; type `licence'     *
   *  for details.                                                    *
   ********************************************************************

>> analyze_scan
##########################################################################
## ANALYZE_SCAN: a routine for batch fitting of ENGIN-X data ########
## For help, type:    analyze_scan/help.                      ########
##########################################################################


#####################################################
######## Please define the type of scan: ##########
#####################################################
 (1) Sequential set of runs
 (2) Custom set of runs from file
 (3) Partial saves
 (4) Sequential set of periods
 (5) Individual detectors from file
 (0) Exit
#####################################################
Please select option [ENTER for default=1]: 1
```


Electronic copy available at: https://ssrn.com/abstract=3711244

Open GENIE

```
   ************************************************************************

>> analyze_scan
########################################################################
## ANALYZE_SCAN: a routine for batch fitting of ENGIN-X data ########
## For help, type:    analyze_scan/help.                      ########
########################################################################


#####################################################
######## Please define the type of scan: ###########
#####################################################
 (1) Sequential set of runs
 (2) Custom set of runs from file
 (3) Partial saves
 (4) Sequential set of periods
 (5) Individual detectors from file
 (0) Exit
#####################################################
Please select option [ENTER for default=1]:
#####################################################
First run [press ENTER for default=10000]: 236826
Last run [press ENTER for default=236826]:
Bank [press ENTER for default=1]:
Reading focussed datafile: C:\Engin-X\focus\ENGINX236826_1.his
############################################################
 The current parameter file doesn't match the one used when
 focussing the run! This means that you will not get absolute
 values of the lattice parameters.
 If you are indeed interested in absolute values,
 please change the calibration by running:

 change_calibration RB_NUMBER

 where RB_NUMBER is the RB_NUMBER of your experiment

 More help? Email to:
 Ed Oliver (E.C.Oliver@rl.ac.uk)
 Javier Santisteban (emoso@yahoo.com)
############################################################
Reading focussed datafile: C:\Engin-X\focus\ENGINX236826_1.his

#####################################################
##       Variables for on-screen plotting:      ##
```


Electronic copy available at: https://ssrn.com/abstract=3711244

Open GENIE

```
##################################################
Please select option [ENTER for default=1]:
##################################################
First run [press ENTER for default=10000]: 236826
Last run [press ENTER for default=236826]:
Bank [press ENTER for default=1]:
Reading focussed datafile: C:\Engin-X\focus\ENGINX236826_1.his
################################################################
 The current parameter file doesn't match the one used when
 focussing the run! This means that you will not get absolute
 values of the lattice parameters.
 If you are indeed interested in absolute values,
 please change the calibration by running:

 change_calibration RB_NUMBER

 where RB_NUMBER is the RB_NUMBER of your experiment

 More help? Email to:
 Ed Oliver (E.C.Oliver@rl.ac.uk)
 Javier Santisteban (emoso@yahoo.com)
################################################################
Reading focussed datafile: C:\Engin-X\focus\ENGINX236826_1.his

##################################################
##       Variables for on-screen plotting:      ##
##################################################
 (0) No plotting
 (1) Run number
 (2) X positioner
 (3) Y positioner
 (4) Z positioner
 (5) OMEGA positioner
 (6) Strain from stress rig
 (7) Stress from stress rig
 (8) Furnace temperature
 (9) External values (from file)
 (-1) Exit
##################################################
Please select option [ENTER for default=0]:
```

PGOLEDriver - PGOLED1

File Edit View Window Help

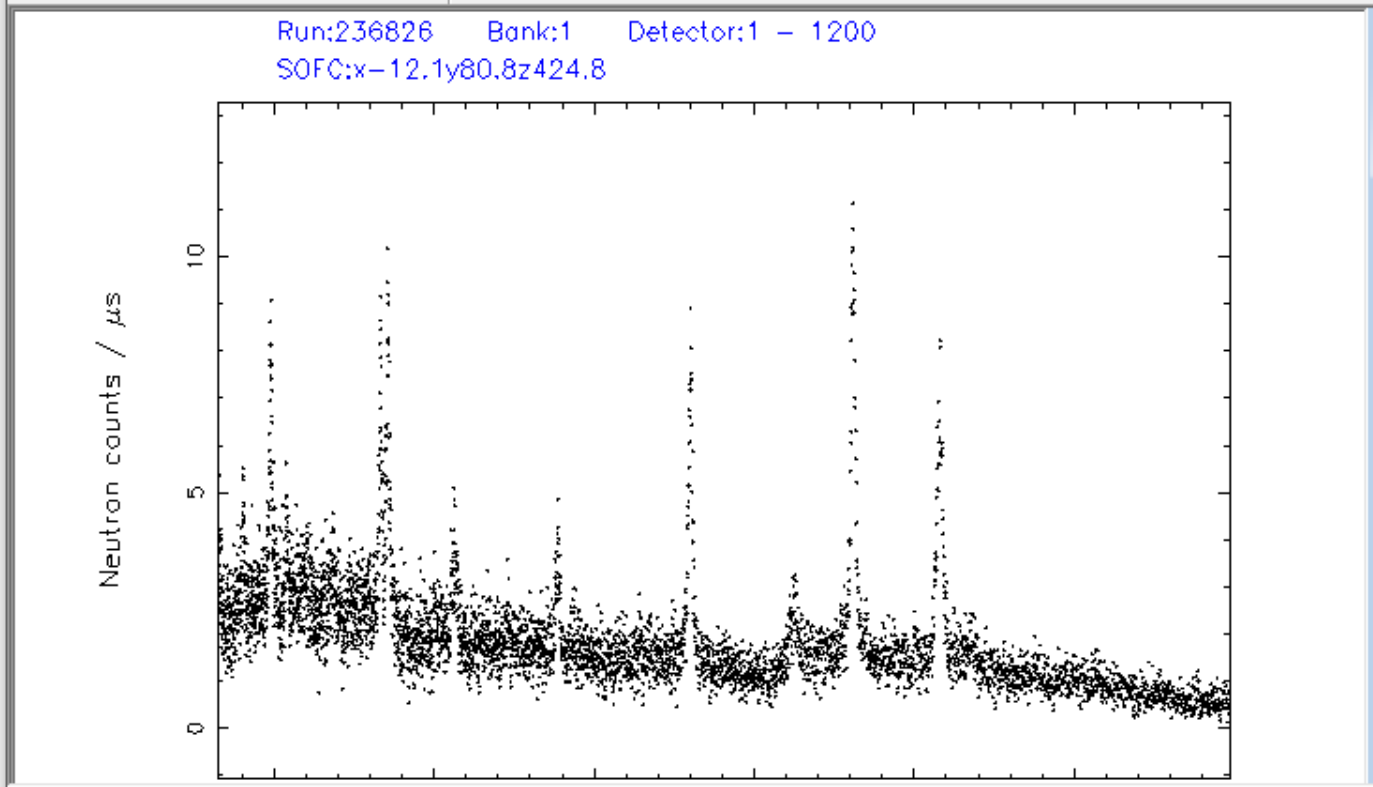

For Help, press F1

Electronic copy available at: https://ssrn.com/abstract=3711244

Open GENIE

```
############################################################
 The current parameter file doesn't match the one used when
 focussing the run! This means that you will not get absolute
 values of the lattice parameters.
 If you are indeed interested in absolute values,
 please change the calibration by running:

 change_calibration RB_NUMBER

 where RB_NUMBER is the RB_NUMBER of your experiment

 More help? Email to:
 Ed Oliver (E.C.Oliver@rl.ac.uk)
 Javier Santisteban (emoso@yahoo.com)
############################################################
Reading focussed datafile: C:\Engin-X\focus\ENGINX236826_1.his

##################################################
##       Variables for on-screen plotting:      ##
##################################################
 (0) No plotting
 (1) Run number
 (2) X positioner
 (3) Y positioner
 (4) Z positioner
 (5) OMEGA positioner
 (6) Strain from stress rig
 (7) Stress from stress rig
 (8) Furnace temperature
 (9) External values (from file)
 (-1) Exit
##################################################
Please select option [ENTER for default=0]:
##################################################
Reading focussed datafile: C:\Engin-X\focus\ENGINX236826_1.his

Please look at the graphics window and decide the TOF range for fitting:

Please give minimum TOF for fitting [press ENTER for default=20000.0]:
Please give maximum TOF for fitting [press ENTER for default=40000.0]:
T_min_ROI was too low, so t_min_ROI was changed to  20000.0
T_max_ROI was too high, so t_max_ROI was changed to  40000.0
Sample not defined - please define the sample
New sample name (a single word, please ?)(q=CANCEL):
```

PGOLEDriver - PGOLED1

File Edit View Window Help

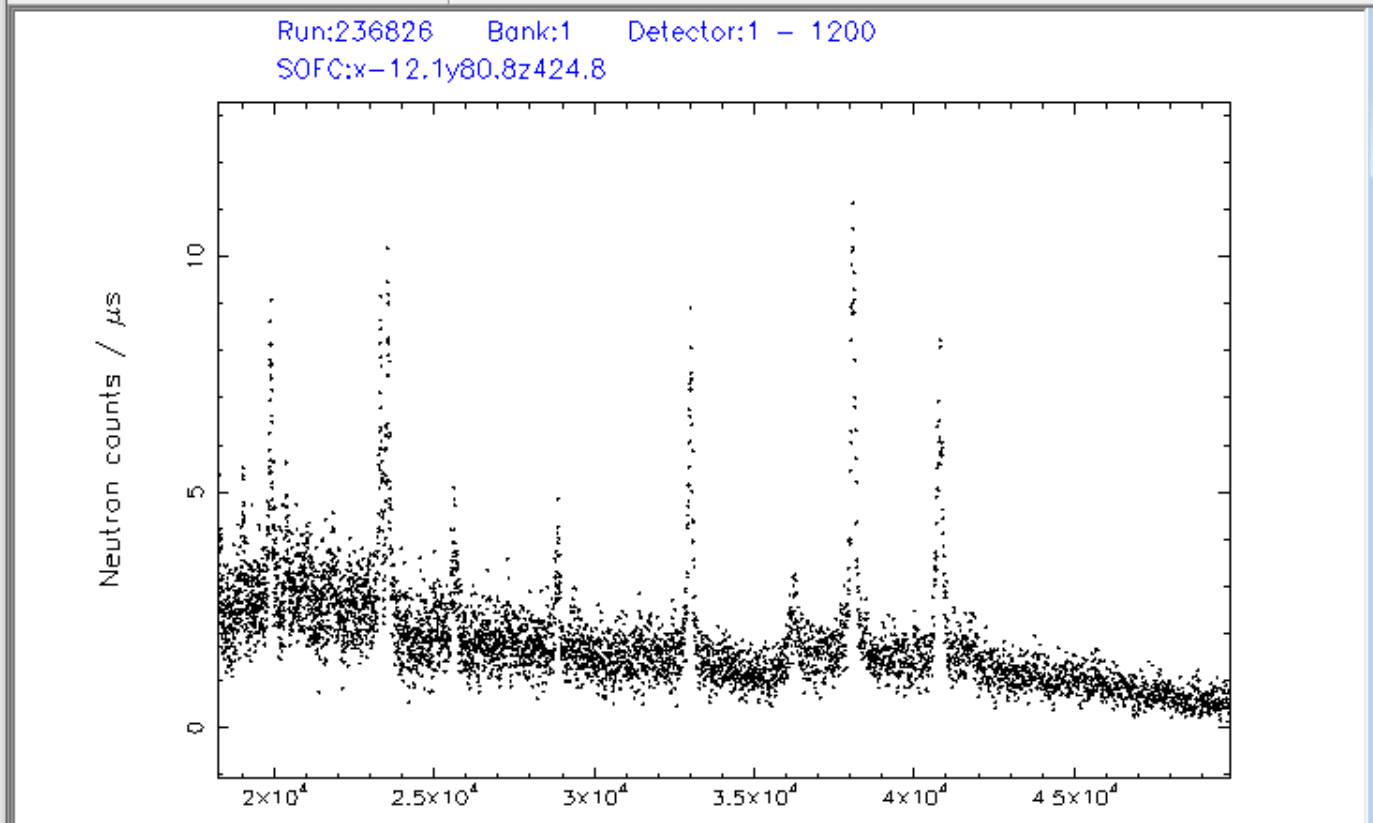

For Help, press F1

Electronic copy available at: https://ssrn.com/abstract=3711244

Open GENIE

```
24/09/2008  16:29             6,068 AG.EXP
24/09/2008  16:29             6,068 AL.EXP
24/09/2008  16:29             6,560 AL2O3_ALPHA.EXP
24/09/2008  16:29             6,068 AU.EXP
24/09/2008  16:29             6,396 BE.EXP
24/09/2008  16:29             7,544 CAF2.EXP
01/06/2009  19:05            11,480 CALCITE.EXP
24/09/2008  16:29             7,544 CEO2.EXP
24/09/2008  16:29             6,806 CO2W6C2.EXP
24/09/2008  16:29             6,806 CO3W9C4.EXP
24/09/2008  16:29             6,806 CO6W6C.EXP
24/09/2008  16:29             6,232 CR.EXP
24/09/2008  16:29             5,986 CU.EXP
24/09/2008  16:29             6,232 FE_ALPHA.EXP
24/09/2008  16:29             6,232 FE_GAMMA.EXP
30/10/2013  16:14             8,692 GAMMA_PRIME_NI3AL.EXP
24/09/2009  00:12             6,314 JoeNI.EXP
24/09/2008  16:29             5,822 LI_BETA.EXP
28/05/2009  19:05             7,380 MG.EXP
24/09/2008  16:29             6,232 MO.EXP
24/09/2008  16:29             6,232 NB.EXP
24/09/2008  16:29             6,232 NI.EXP
09/06/2014  18:01            20,008 NiMnGa_cubic.EXP
24/09/2008  16:29             6,232 NI_GAMMA.EXP
29/11/2012  12:39             6,314 NI_gamma_new.EXP
24/09/2008  16:29             6,232 NI_GAMMA_P.EXP
24/09/2008  16:29             6,068 PB.EXP
24/09/2008  16:29             6,068 PT.EXP
24/09/2008  16:29             6,068 SI.EXP
24/09/2008  16:29             7,790 SIC_ALPHA.EXP
24/09/2008  16:29             6,806 SIC_BETA.EXP
24/09/2008  16:29             5,740 SN_ALPHA.EXP
24/09/2008  16:29             6,724 SN_BETA.EXP
26/09/2013  15:47             8,528 TIAL.EXP
24/09/2008  16:29             6,232 TI_ALPHA.EXP
24/09/2008  16:29             7,052 TI_BETA.EXP
24/09/2008  16:29             6,888 U_ALPHA.EXP
24/09/2008  16:29             6,068 W.EXP
24/09/2008  16:29             6,314 W2C.EXP
24/09/2008  16:29             7,626 WC.EXP
24/09/2008  16:29             6,232 ZR_ALPHA.EXP
              41 File(s)        288,722 bytes
               0 Dir(s)  207,741,730,816 bytes free
Phase 1: please choose phase from above list (e.g: Fe_alpha, without .exp):
```

PGOLEDriver - PGOLED1

File Edit View Window Help

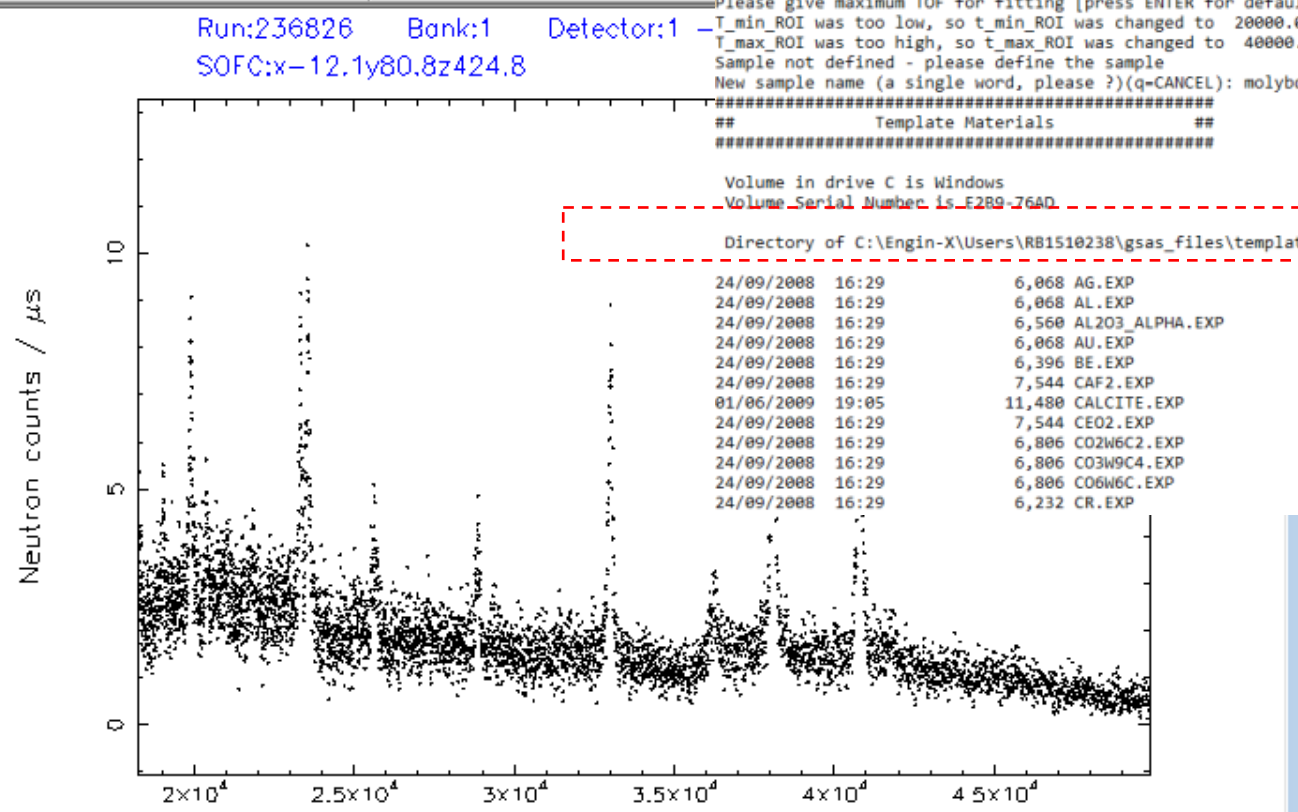

For Help, press F1

Open GENIE

```
################################################
Reading focussed datafile: C:\Engin-X\focus\ENGINX236826_1.his

Please look at the graphics window and decide the TOF range for fitting:

Please give minimum TOF for fitting [press ENTER for default=20000.0]:
Please give maximum TOF for fitting [press ENTER for default=40000.0]:
T_min_ROI was too low, so t_min_ROI was changed to  20000.0
T_max_ROI was too high, so t_max_ROI was changed to  40000.0
Sample not defined - please define the sample
New sample name (a single word, please ?)(q-CANCEL): molybdenum
################################################
##              Template Materials              ##
################################################

 Volume in drive C is Windows
 Volume Serial Number is F2B9-76AD

 Directory of C:\Engin-X\Users\RB1510238\gsas_files\templates

24/09/2008  16:29             6,068 AG.EXP
24/09/2008  16:29             6,068 AL.EXP
24/09/2008  16:29             6,560 AL2O3_ALPHA.EXP
24/09/2008  16:29             6,068 AU.EXP
24/09/2008  16:29             6,396 BE.EXP
24/09/2008  16:29             7,544 CAF2.EXP
01/06/2009  19:05            11,480 CALCITE.EXP
24/09/2008  16:29             7,544 CEO2.EXP
24/09/2008  16:29             6,806 CO2W6C2.EXP
24/09/2008  16:29             6,806 CO3W9C4.EXP
24/09/2008  16:29             6,806 CO6W6C.EXP
24/09/2008  16:29             6,232 CR.EXP
```


Electronic copy available at: https://ssrn.com/abstract=3711244

Open GENIE

```
24/09/2008  16:29             6,232 CR.EXP
24/09/2008  16:29             5,986 CU.EXP
24/09/2008  16:29             6,232 FE_ALPHA.EXP
24/09/2008  16:29             6,232 FE_GAMMA.EXP
30/10/2013  16:14             8,692 GAMMA_PRIME_NI3AL.EXP
24/09/2009  00:12             6,314 JoeNI.EXP
24/09/2008  16:29             5,822 LI_BETA.EXP
28/05/2009  19:05             7,380 MG.EXP
24/09/2008  16:29             6,232 MO.EXP
24/09/2008  16:29             6,232 NB.EXP
24/09/2008  16:29             6,232 NI.EXP
09/06/2014  18:01            20,008 NiMnGa_cubic.EXP
24/09/2008  16:29             6,232 NI_GAMMA.EXP
29/11/2012  12:39             6,314 NI_gamma_new.EXP
24/09/2008  16:29             6,232 NI_GAMMA_P.EXP
24/09/2008  16:29             6,068 PB.EXP
24/09/2008  16:29             6,068 PT.EXP
24/09/2008  16:29             6,068 SI.EXP
24/09/2008  16:29             7,790 SIC_ALPHA.EXP
24/09/2008  16:29             6,806 SIC_BETA.EXP
24/09/2008  16:29             5,740 SN_ALPHA.EXP
24/09/2008  16:29             6,724 SN_BETA.EXP
26/09/2013  15:47             8,528 TIAL.EXP
24/09/2008  16:29             6,232 TI_ALPHA.EXP
24/09/2008  16:29             7,052 TI_BETA.EXP
24/09/2008  16:29             6,888 U_ALPHA.EXP
24/09/2008  16:29             6,068 W.EXP
24/09/2008  16:29             6,314 W2C.EXP
24/09/2008  16:29             7,626 WC.EXP
24/09/2008  16:29             6,232 ZR_ALPHA.EXP
              41 File(s)        288,722 bytes
               0 Dir(s)  207,741,730,816 bytes free
Phase 1: please choose phase from above list (e.g: Fe_alpha, wit
Sample temperature (K) [press ENTER for default=293K]:
STOP EXPEDT terminated successfully statement executed
Sample properties stored in enginX.sample
###### Calculating PHASE=1 -- BANK=1 ########
STOP EXPEDT terminated successfully statement executed
        1 file(s) copied.

################################################
The present sample is molybdenum

Do you want to change to a different sample? (y/n, press ENTER for default=n):
```

PGOLEDriver - PGOLED1

File Edit View Window Help

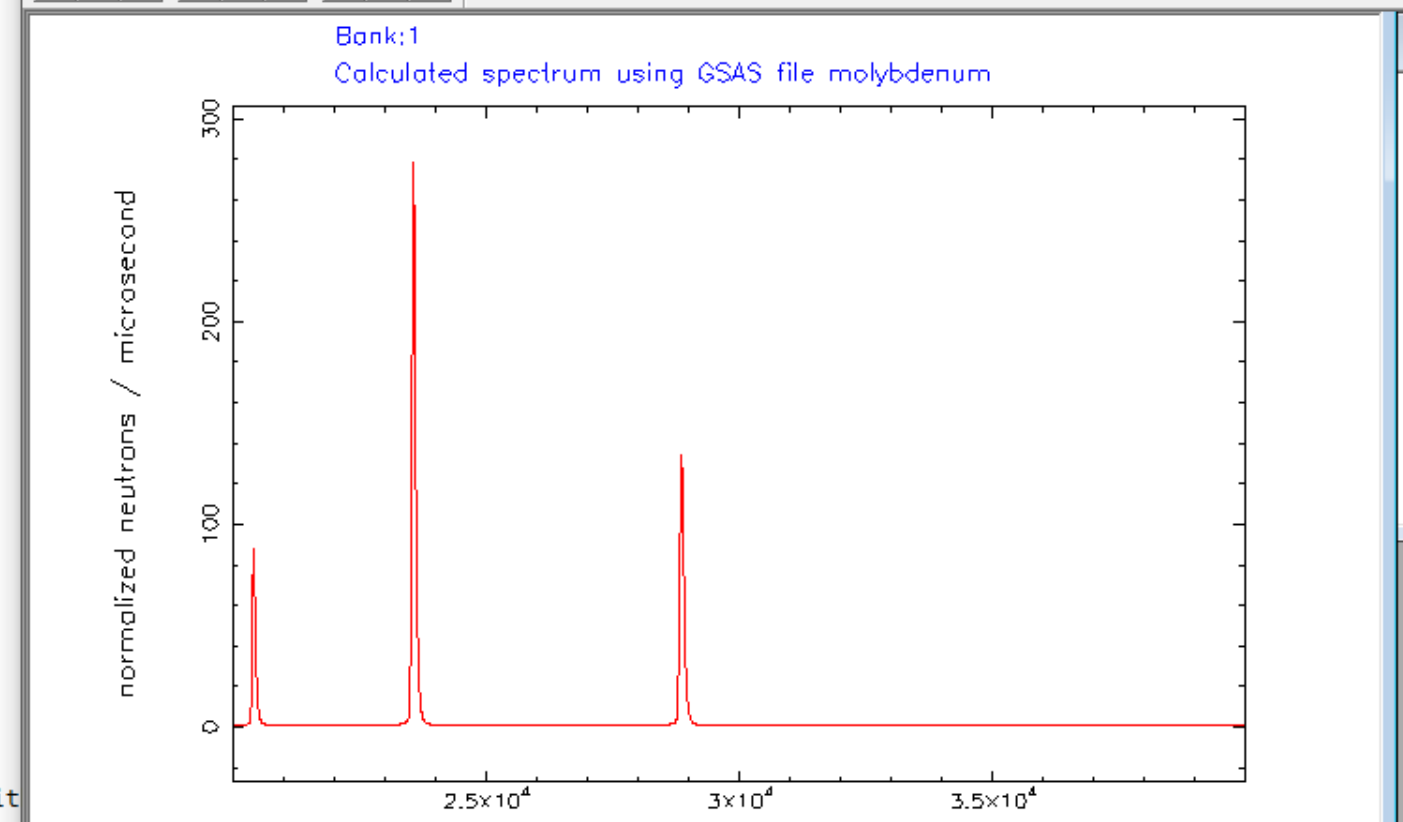

For Help, press F1

Electronic copy available at: https://ssrn.com/abstract=3711244

Open GENIE

```
24/09/2008  16:29             6,232 TI_ALPHA.EXP
24/09/2008  16:29             7,052 TI_BETA.EXP
24/09/2008  16:29             6,888 U_ALPHA.EXP
24/09/2008  16:29             6,068 W.EXP
24/09/2008  16:29             6,314 W2C.EXP
24/09/2008  16:29             7,626 WC.EXP
24/09/2008  16:29             6,232 ZR_ALPHA.EXP
              41 File(s)        288,722 bytes
               0 Dir(s)  207,741,730,816 bytes free
Phase 1: please choose phase from above list (e.g: Fe_alpha, wit
Sample temperature (K) [press ENTER for default=293K]:
STOP EXPEDT terminated successfully statement executed
Sample properties stored in enginX.sample
###### Calculating PHASE=1 -- BANK=1 ########
STOP EXPEDT terminated successfully statement executed
        1 file(s) copied.

##################################################
The present sample is molybdenum

Do you want to change to a different sample? (y/n, press ENTER f
###### Calculating PHASE=1 -- BANK=1 ########
STOP EXPEDT terminated successfully statement executed
        1 file(s) copied.
scale factor=
0.000310819345997
##################################################
##################################################
 The current sample is molybdenum
 The min TOF to be used in the analysis is 20000.0
 The max TOF to be used in the analysis is 40000.0
 There are 2 reflections within this range
 The lowest hkl reflection in this range is (2,0,0)  at  28830.0
 The highest hkl reflection in this range is (2,1,1)  at  23540.
 The highest intensity peak (assuming random texture) is (2,1,1)
##################################################
Pawley fitting, free gamma, and peak 4 as seed
Reading focussed datafile: C:\Engin-X\focus\ENGINX236826_1.his
SYSTEM: system() returned unusual status = 3
SYSTEM: executed command was "C:\WINDOWS\system32\cmd.exe /c "genles 236826_1 > nul 2> nul""
 Refinement did not converge!
Are you happy with this fit? (y=continue, n=exit, press ENTER for default=y):
```

PGOLEDriver - PGOLED1

File Edit View Window Help

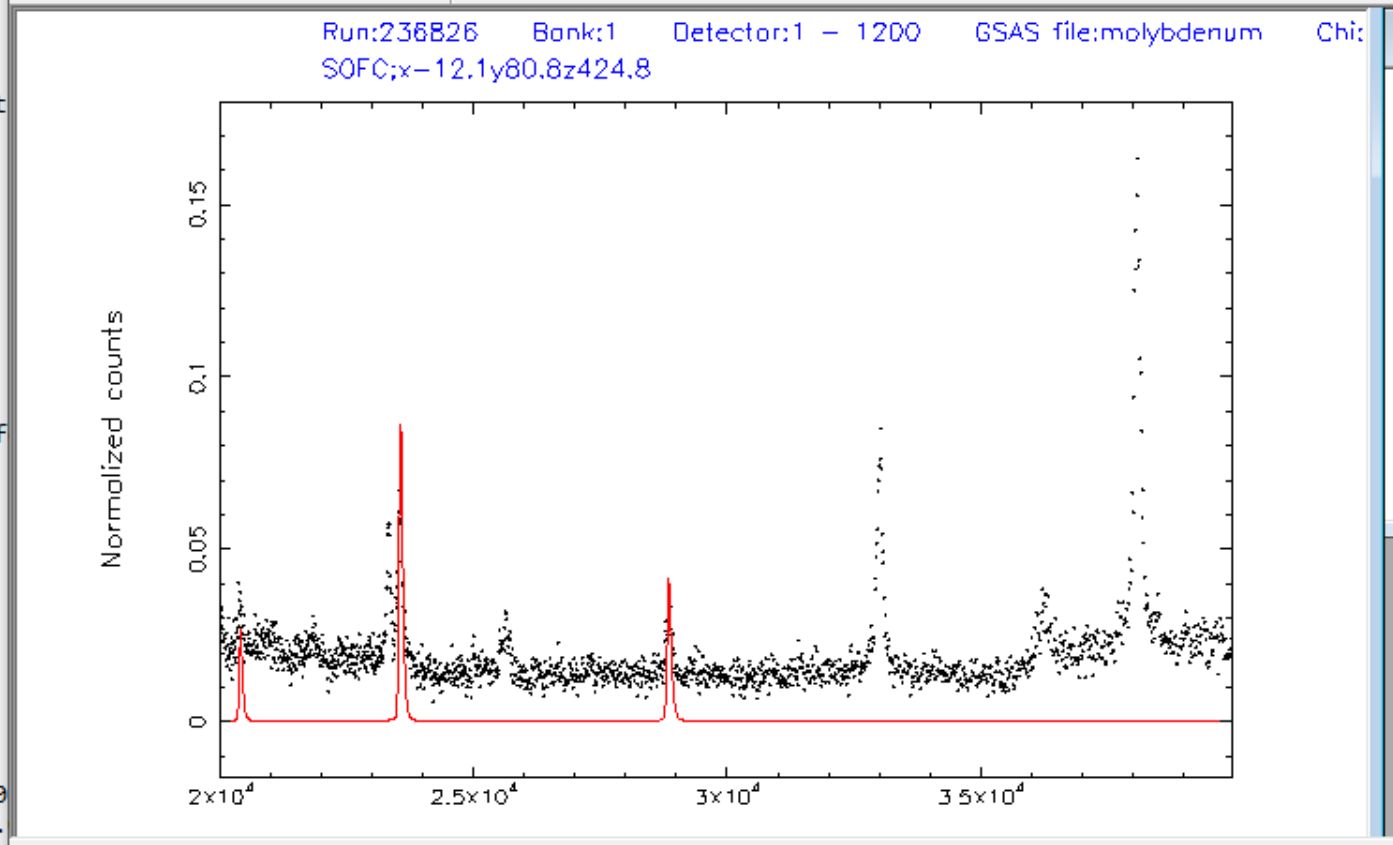

For Help, press F1

Electronic copy available at: https://ssrn.com/abstract=3711244

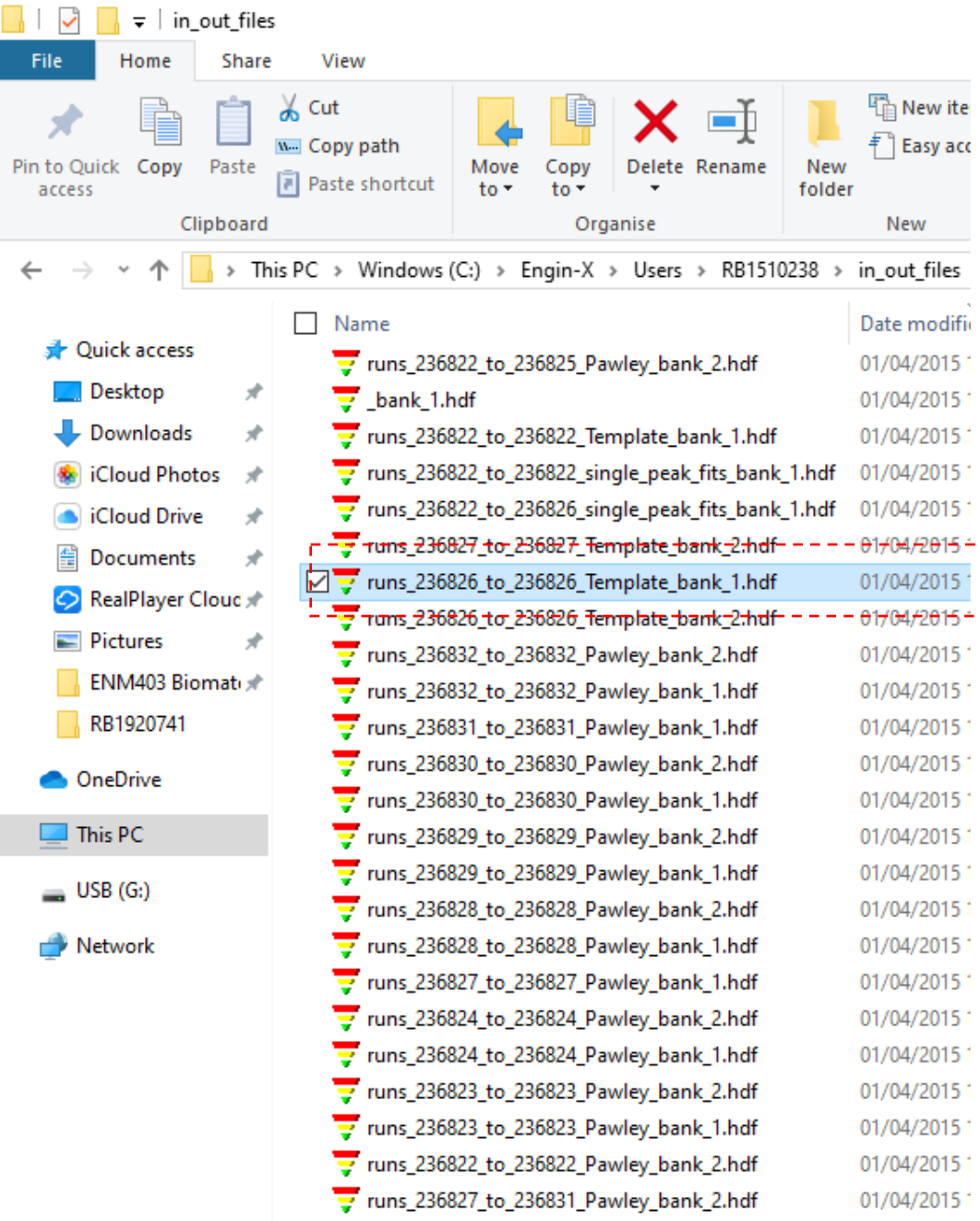

The d-spacing value and the error saved in HDF software

Electronic copy available at: https://ssrn.com/abstract=3711244

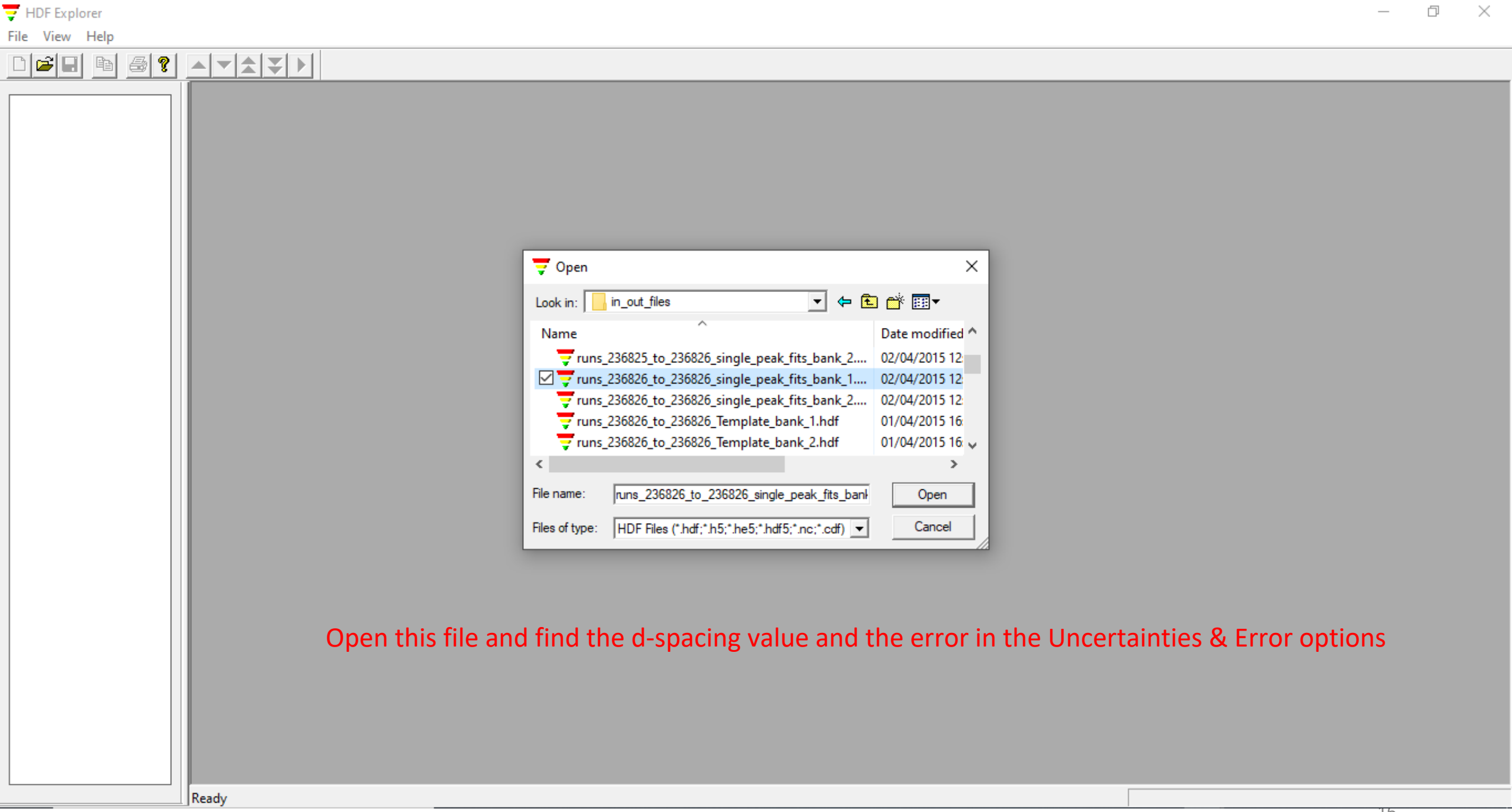

Open this file and find the d-spacing value and the error in the Uncertainties & Error options

Electronic copy available at: https://ssrn.com/abstract=3711244